Title
PINs lost and PINs gained: Auxin-transport mediated patterning in the grasses

Author
O'Connor, Devin Lee

Publication Date
2012

Peer reviewed|Thesis/dissertation

PINs lost and PINs gained: Auxin-transport mediated patterning in the grasses

By
Devin Lee O'Connor

A dissertation submitted in partial satisfaction of the
requirements for the degree of
Doctor of Philosophy
in
Plant Biology
in the
Graduate Division
of the
University of California, Berkeley

Committee in charge:

Professor Sarah C. Hake, Chair
Professor Jay B. Hollick
Professor Nipam H. Patel
Professor Chelsea D. Specht

Spring 2012

Abstract

PINs lost and PINs gained: Auxin-transport mediated patterning in the grasses

by

Devin Lee O'Connor

Doctor of Philosophy in Plant Biology

University of California, Berkeley

Professor Sarah Hake, Chair

In plants, transport mediated by the PINFORMED (PIN) family of auxin efflux carriers helps create gradients on which many developmental processes depend. Current models suggest that *Arabidopsis* PIN1 has two concurrent functions during leaf initiation: 1) concentrating auxin to create local maxima in the meristem epidermis, and 2) transporting auxin away from the epidermal maxima and into the internal tissues. The resulting auxin gradient is required for leaf initiation and vein patterning. I identified an angiosperm *PIN* clade placed sister to *PIN1*, here termed *Sister-of-PIN1* (*SoPIN1*), that has likely been lost within the *Brassicaceae*, including in *Arabidopsis*, but remains in all other angiosperms sampled. I also identify a conserved duplication of *PIN1* to create *PIN1a* and *PIN1b* within the grasses. I used live-cell imaging and immuno-localization to characterize the expression and localization of SoPIN1, PIN1a and PIN1b members in both maize and *Brachypodium*. SoPIN1 expression is highest in the epidermis and is consistently oriented toward areas where the DR5 auxin reporter is highly expressed, suggesting that SoPIN1 functions in the creation of auxin maxima. PIN1a and PIN1b localization, largely absent from the epidermis and oriented rootward in the internal tissues, suggests that these PIN proteins transport auxin after maxima formation during the canalization of leaf and stem veins. These data support the functional division of PIN proteins into maxima creation and canalization modes. In addition, the loss of *SoPIN1* within the *Brassicaceae* suggests that PIN1 in this group may be unique amongst the angiosperms in its ability to dynamically switch between these two functional modes. I then provide a model for how the *PIN1a/PIN1b* duplication in the lineage leading to the grasses may relate to the novel morphological and anatomical characteristics found in monocot plants. Finally, I summarize some preliminary *PIN* knockdown experiments that suggest a role for PIN mediated patterning in apical dominance, meristem maintenance and leaf proximal/distal patterning.

Table of Contents

Dedication

This work is dedicated to my parents Edie and Greg O'Connor, who are unfailing in their support, generosity and love.

Acknowledgments

Thanks to Sarah for being my mentor and my inspiration. Thanks to my committee who have provided valuable and constructive discussions of the years. Thanks to my many undergraduate helpers, who have seen me through highs and lows, Ranjani Lakshmin, Steven Sun, Margaret Taylor, Scott Hirose, and Connie Lee. Thanks to all the members of the Hake lab for being such enjoyable and intelligent people to work with. Special thanks to Nathalie Bolduc and George Chuck who have seen me through it all. Thanks to Aaron Sluis for taking up the torch of PIN proteins in the Hake lab. I couldn't have done many of these experiments without collaborating with several members of the Vogel lab at the USDA-ARS. Special thanks to John Vogel, Jenn Bragg, Rita Nieu, and Alana Clark. Thanks to David Jackson, for many valuable materials as well as valuable discussions. To Andrea Gallavotti for the DR5 construct. To Anna Bates at the USDA confocal. To the greenhouse staff. I must thank my crew of friends, for many great adventures, distractions, support, guidance, and inspiration. The Big Jerm, 'lanes, C-Money, Katester, "The Wall", and KK, gonna miss you all. Finally a big thanks to the love of my life, and my-soon-to-be wife, Hayley.

Introduction

The diversity of plant form may seem to stand in defiance of a unified developmental explanation. Yet a long history of theories attempts to simplify this morphological diversity as the product of distinct evolutionary stages and developmental modules. In 1879 Asa Gray described the “phytomer”, a basic developmental module consisting of a section of stem, leaf, and branch that is still relevant to current research (Gray 1879). In 1952, based on early vascular plant fossils consisting of a simple equally-branching stem-like axis, Walter Zimmerman proposed that all vascular plant organs, including the parts of the phytomer, evolved from the alteration of a single ancestral organ, the telome (Zimmermann 1952). Today much work is devoted to how the active cell-to-cell transport of the plant hormone auxin controls plant shape. The modular and self organizing nature of auxin transport likely provides developmental robustness and flexibility to accommodate the sessile nature of plants, but also provides a malleable scaffold for morphological evolution.

Most models of auxin-transport mediated patterning propose that auxin freely diffuses into cells, but once ionized inside, is not able to diffuse out (Raven 1975; Rubery and Sheldrake 1973; 1974). Thus, of the numerous auxin transport proteins (For review see Petrásek and Friml 2009), auxin export, mediated by membrane localized PIN-FORMED (PIN) proteins, appears to be the rate-limiting step in the directional movement of auxin in many contexts (Petrásek et al. 2006; Wisniewska et al. 2006). The gradient of auxin created by polar localization of PIN is one of the earliest indications of polarity within a tissue and creates basic positional information on which a myriad of other developmental and physiological processes depend (Chen et al. 1998; Friml et al. 2002; Friml et al. 2003; Friml et al. 2002; Luschnig et al. 1998; Müller et al. 1998; Okada et al. 1991).

Localization and genetic studies have identified PIN1 (AtPIN1) as the major auxin transporter involved in leaf initiation and vascular development in the above-ground tissues (Benková et al. 2003; Reinhardt et al. 2003; Scarpella et al. 2006). The current model for how PIN1-mediated auxin transport establishes tissue and cell patterning within the plant consists of two main parts. First, the “canalization hypothesis” presumes that auxin positively regulates its own movement in the direction of the dominant flux, and thus any auxin maximum can quickly become a narrow “canalized” auxin stream (Sachs 1991; 1969). Canalization events occur between areas of high auxin concentration, called source tissues, to areas of low auxin concentration, called sink tissues. Second, the “convergence point hypothesis” posits that it is the creation of epidermal auxin maxima in the outer cell layer of the plant (L1) by PIN1 that defines the location of initiating leaves and leaf vasculature (Reinhardt et al. 2003; Scarpella et al. 2006; Reinhardt et al. 2000). The sites where auxin maxima form are defined by PIN1 ”convergence points", where PIN1 is convergently localized and thus directs auxin into a few cells in the L1.

The grass family is likely the most essential plant group to human survival. Cereals provide more than 50% of human caloric intake world-wide and dedicated biomass grasses such as *Miscanthus* and switchgrass will likely become an important source of biomass for renewable energy production (Somerville 2006). The ecological importance of grasses should also be acknowledged as it is estimated that they cover 1/3 of the arable land on earth (Shantz 1954). Yet despite their importance, our understanding of grass developmental patterning is lacking, especially in regards to the leaf.

This work utilizes both maize and the new model grass *Brachypodium distachyon. Brachypodium* is a wild temperate grass that is sister to agriculturally important temperate species such as wheat, oats, and barley (Vogel et al. 2006) and is a member of the *Pooideae*, a group that contains more species than any other grass sub-family (Kellogg 2001). In addition to genomic resources including microarrays, T-DNA mutant lines, and small RNA data, *Brachypodium* has other practical advantages due to its short generation time, small size, ease of growth, and a self-fertile breeding strategy (Draper et al. 2001). But above all, *Brachypodium* has the potential to become one of the most influential grass models because of the efficiency and relative ease of genetic transformation (Vogel and Hill 2008; Vain et al. 2008).

This thesis focuses on how PIN proteins act during the development of the grass vegetative and floral tissues. In Chapter 1, I present the most comprehensive phylogenetic analysis of angiosperm PIN proteins to date. I provide evidence that *Arabidopsis* has lost a clade of PIN proteins that is conserved in all other Angiosperms sampled and that differences in PIN function in the grasses may be due to either changes in transcription or protein sequence. In Chapter 2, my characterization of the expression and localization of several PIN proteins in grasses provides further support that a functional division may exist in land plant PIN proteins between concentrating auxin up the gradient during maxima formation and canalizing auxin with-the-flux during vein patterning. In Chapter 3, I suggest that a *PIN* gene duplication conserved in grasses may help explain some of the fundamental developmental differences between two of the largest monophyletic angiosperm groups, the eudicots and the monocots. Finally, in Chapter 4, I use reverse genetics and chemical treatments to begin to understand the functional significance of PIN proteins in grass development. Combined, this work provides valuable insight into how differences in gene family structure between groups, as well as changes in auxin-transport mediated patterning may help explain the evolution of novel traits.

Chapter 1: Phylogenetic and Genomic Analysis of the Angiosperm Long-PINs

Introduction

PIN proteins contain two trans-membrane regions separated by a variable internal hydrophilic loop, the length of which allows the family to be divided into two broad classes (See Krecek et al. 2009 for review). The "Short" PIN proteins have a short hydrophilic region and include *Arabidopsis* PIN5, PIN6 and PIN8 (Krecek et al. 2009). Short-PINs are localized to the endoplasmic reticulum and are likely involved in auxin homoeostasis within the cell (Mravec et al. 2009). PIN proteins with a long hydrophilic region are referred to as "Long" PINs. *Arabidopsis* Long-PINs include PIN1, PIN2, and the closely related clade of PIN3, PIN4, and PIN7 (Bayer et al. 2009; Blilou et al. 2005; Reinhardt et al. 2003). Previous phylogenetic analyses support the division of the PIN family into Long and Short PIN clades as well as an expansion of the PIN family in the angiosperms (Krecek et al. 2009; Paponov et al. 2005). However, most previous phylogenies have only sampled a limited number of angiosperms and have very poor support.

Long-PINs show a characteristic polar localization in the cell plasma membrane that provides directionality to auxin transport (Benková et al. 2003; Blilou et al. 2005; Friml et al. 2003; Reinhardt et al. 2003; Scarpella et al. 2006). The hydrophilic loop domains of Long-PIN proteins contain phosphorylation sites that control PIN cellular localization (Dhonukshe et al. 2010; Huang et al. 2010; Zhang et al. 2010). Thus it is likely that variation in function between PIN family members is at least in part due to differing protein domains within this region. In the *Arabidopsis* root the overlapping expression domains of several PINs make up an auxin transport path that maintains an auxin gradient in the root tip (Blilou et al. 2005). Thus the transcriptional regulation of PINs across the family is likely important to their differing functions as well.

Because of the highly documented importance of Long-PINs in developmental patterning I focused my phylogenetic analysis on this subgroup within the PIN family. In this chapter I use phylogenetic analysis to identify the basic family structure within the angiosperm Long-PINs. In addition I examine to what degree the protein sequences of the hydrophilic loops and putative regulatory regions may differ between members of the Long-PIN group.

Results

The Long-PIN Family in the Angiosperms

My phylogenetic analysis of Long-PIN sequences sampled from across the land plants supports a diversification of the Long-PINs within angiosperms (Figure 1). All angiosperm sequences form a single group while sequences from the more

basal land plants, *Physcomitrella patens* and *Selaginella moellendorffii*, are separate (Figure 1B). Further sampling within non-angiosperm groups is needed, but with the available data, my analysis supports the presence of a single canonical Long-PIN protein in the ancestor of these land plants.

Within the angiosperms sampled, I identified four highly supported *Long-PIN* clades (Figure 1B). All sampled angiosperms contain sequences that nested with *Arabidopsis thaliana* PIN1, PIN2, and PIN3/4/7 sequences. Thus these clades were designated "PIN1", "PIN2" and "PIN3,4,7", respectively (Figure 1B). My analysis supports a fourth clade within the angiosperms placed sister to the PIN1 clade, here designated "Sister-of-PIN1" (SoPIN1). The *SoPIN1* clade contains sequences from all sampled angiosperms with the exception of species within the *Brassicaceae,* including *Brassica rapa*, *Arabidopsis lyrata* and *Arabidopsis thaliana* (Figure 1A). This topology suggests that *SoPIN1* was lost in the lineage leading to the *Brassicaceae* after their divergence from *Papaya*.

I provided further support for the loss of *SoPIN1* in the *Brassicaceae* lineage by examining the synteny of genes surrounding *SoPIN1* across a subset of angiosperms with whole genome sequences. I identified strong synteny in the *SoPIN1* region across many eudicots and weaker synteny between several eudicots and rice (Figure 2). However, *SoPIN1* is absent in the syntenic chromosomes of *A. thaliana* and *Brassica rapa,* both members of the *Brassicaceae,* despite conservation of the neighboring genes. These data provide strong support that *A. thaliana* and other members of the *Brassicaceae* have lost one of the four canonical *Long-PINs* clades conserved in all other angiosperms.

In previous work SoPIN1 proteins were annotated as PIN1 orthologs (Bayer et al. 2009; Brooks et al. 2009; Peng and Chen 2011). However, in addition to my phylogenetic analysis that positions *SoPIN1* in a unique clade, I identified several conserved regions within the variable cytosolic loop of SoPIN1 proteins that are not found in members of the PIN1 clade (Figure 3: red box). Furthermore, SoPIN1 proteins lack regions that are conserved in the PIN1 clade (Figure 3: blue boxes). Thus while SoPIN1 proteins are very similar to PIN1 proteins, I hypothesize that they may have unique protein domains that effect their function.

Within the grasses, I identified a lineage-specific duplication event in the PIN1 clade. All grasses sampled contain at least one protein within two PIN1 subclades, termed PIN1a and PIN1b based on previous work in maize (Figure 1: B) (Carraro et al. 2006; Gallavotti et al. 2008). In addition, in maize there is a subsequent duplication of PIN1b to give PIN1c, which based on synteny is likely a retained duplicate from the maize tetraploidy (data not shown). Overall, both PIN1a and PIN1b resemble other eudicot PIN1 proteins, but in some regions of the variable cytosolic loop, PIN1a and PIN1b have grass specific sequences (Figure 3). Because the grasses retained both proteins following the ancient duplication, it is possible that PIN1a and PIN1b have evolved unique functions.

In order to examine how transcriptional regulation may relate to functional differences between members of the PIN1 and SoPIN1 clades, I looked for conserved non-coding sequences (CNS) in the promoter regions of these genes across the grasses. CNS domains are often enriched for known DNA binding motifs and in many cases are conserved because they have important regulatory functions for adjacent genes (Freeling and Subramaniam 2009; Inada 2003; Kaplinsky et al. 2002). I was able to identify several different sequences that are conserved across syntenous orthologs of SoPIN1 (Figure 4), PIN1a (Figure 5) and PIN1b/c (Figure 6). However I was unable to find common CNSs across all three groups (data not shown). These results suggest that members of the SoPIN1, PIN1a and PIN1b clades may have differing transcriptional regulation, and that this may contribute to their differing functions.

Discussion

My phylogenetic analysis supports four major clades within the Angiosperm Long-PIN group, one of which, *SoPIN1* has been lost in the *Brassicaceae.* In general, most angiosperms have a set of four canonical Long-PINs, namely, *PIN1*, *SoPIN1*, *PIN2* and *PIN3,4,7*. However, lineage specific expansion within each subclade is common, suggesting that there may be considerable diversity in PIN functions across the angiosperms.

It is unclear why previous phylogenies failed to identify *SoPIN1* as a unique clade. One possibility is that the gross variation in the GC content between monocot and eudicot sequences in the third codon position falsely skewed previous phylogenies, and monocots and eudicots tended to nest as separate groups (see methods). Another possibility is that previous work assumed a bias towards *Arabidopsis* as a model system. Indeed, some previous phylogenies supported *SoPIN1* as a unique clade sister to PIN1 but still annotated *SoPIN1* members as PIN1 proteins (Zhou et al. 2011; Mravec et al. 2009). Alternatively, my phylogeny includes more non-*Brassicaceae* eudicot species than previous analyses, which gives greater support for a unique *SoPIN1* clade containing both eudicot and monocot members. Regardless, these data strongly support the identification of *SoPIN1* as a unique clade.

My analysis of *SoPIN1*, *PIN1a* and *PIN1b* in the grasses show that all three groups have conserved differences in the variable hydrophilic region as well as conserved CNS domains. Thus it is possible that each group has conserved differences in both cellular localization as well as transcriptional regulation. While species-specific duplication events have occurred in SoPIN1 in rice and *Setaria*, and in PIN1b in maize, *Brachypodium* and *Sorghum* contain single members within the *PIN1a*, *PIN1b* and *SoPIN1* clades. The relationship of *Brachypodium SoPIN1*, *PIN1a* and *PIN1b* to *Arabidopsis PIN1* is summarized in Figure 1: C. My subsequent work focuses on the analysis of these three PINs in *Brachypodium.*

Materials and Methods

Phylogenetic Analysis

PIN coding sequences were gathered from Phytozome (http://www.phytozome.org/) and NCBI (http://www.ncbi.nlm.nih.gov/) using BLAST, and from CoGe (http://synteny.cnr.berkeley.edu/CoGe) (Lyons and Freeling 2008) using synteny. Sequences were analyzed with Geneious. Coding sequences were initially aligned using the putative translation then trimmed. Preliminary phylogenetic analyses were performed with the putative protein translations (Data not shown). While these analyses showed the same overall topology as my final phylogeny, the protein sequences had fewer informative characters and thus lower support. Contrary to results with protein sequences, analysis using the complete coding sequences resulted in a topology where most monocot sequences nested in a single clade. The GC content of the third base of all Monocot sequences (60%) was much higher than eudicot sequences (45%) indicating a probable source of bias. Thus the third base was removed resulting in a more normalized GC content between groups, 33% in monocots vs 30.2% in eudicots. After further alignment with MUSCLE, hyper-variable and unalignable regions were removed. Phylogenetic analysis was performed with MrBayes on the GreenButton service using the Jukes and Cantor model of evolution. 4 chains were run until convergence at 1013000 generations with a standard deviation below 0.01 and sampled every 200 generations. 25% of trees were discarded as burnin. *Physcomatrella* (*P. patens* - Pp1s10_17V6.1 - FUNA) was used as an outgroup.

SoPIN1 Synteny Analysis

BLAST searches of sequenced *Brassicaceae* species using both DNA and protein sequences of *SoPIN1* clade members identified only *Brassicaceae* members of the PIN1 clade. In order to identify the syntenic region corresponding to *SoPIN1* in *Brassicaceae* species, the sequence for a gene neighboring *SoPIN1* in *Papaya* was used to identify the putative *SoPIN1* neighboring gene in *Arabidopsis* (AT2G26800). CoGe (http://synteny.cnr.berkeley.edu/CoGe) synteny analysis using this gene identified syntenic chromosomes across the angiosperms, all of which contained *SoPIN1* except for chromosomes from members of the *Brassicaceae.* Shown in Figure 2 are *Arabidopsis thaliana* and *Brassica rapa*. Synteny was partially preserved between both the alpha and beta genomes of *A. thaliana,* which has undergone multiple tetraploidy events since diverging from *Papaya* (Freeling 2009), but *SoPIN1* was absent from both syntenic chromosomes.

CNS analysis

First, the syntenic chromosomes of *SoPIN1, PIN1a and PIN1b* were identified across the grasses using the BlastX algorithm in CoGe. Then CoGe analysis was

limited to the upstream and downstream regions around each gene. Finally the analysis was run again using the BlastN algorithm in CoGe which is optimized to identify small highly similar CNS sequences. BlastN high scoring pairs (HSPs) that were conserved across most or all of the grasses analyzed were considered CNAs and were manually marked to show their relative locations.

Figures

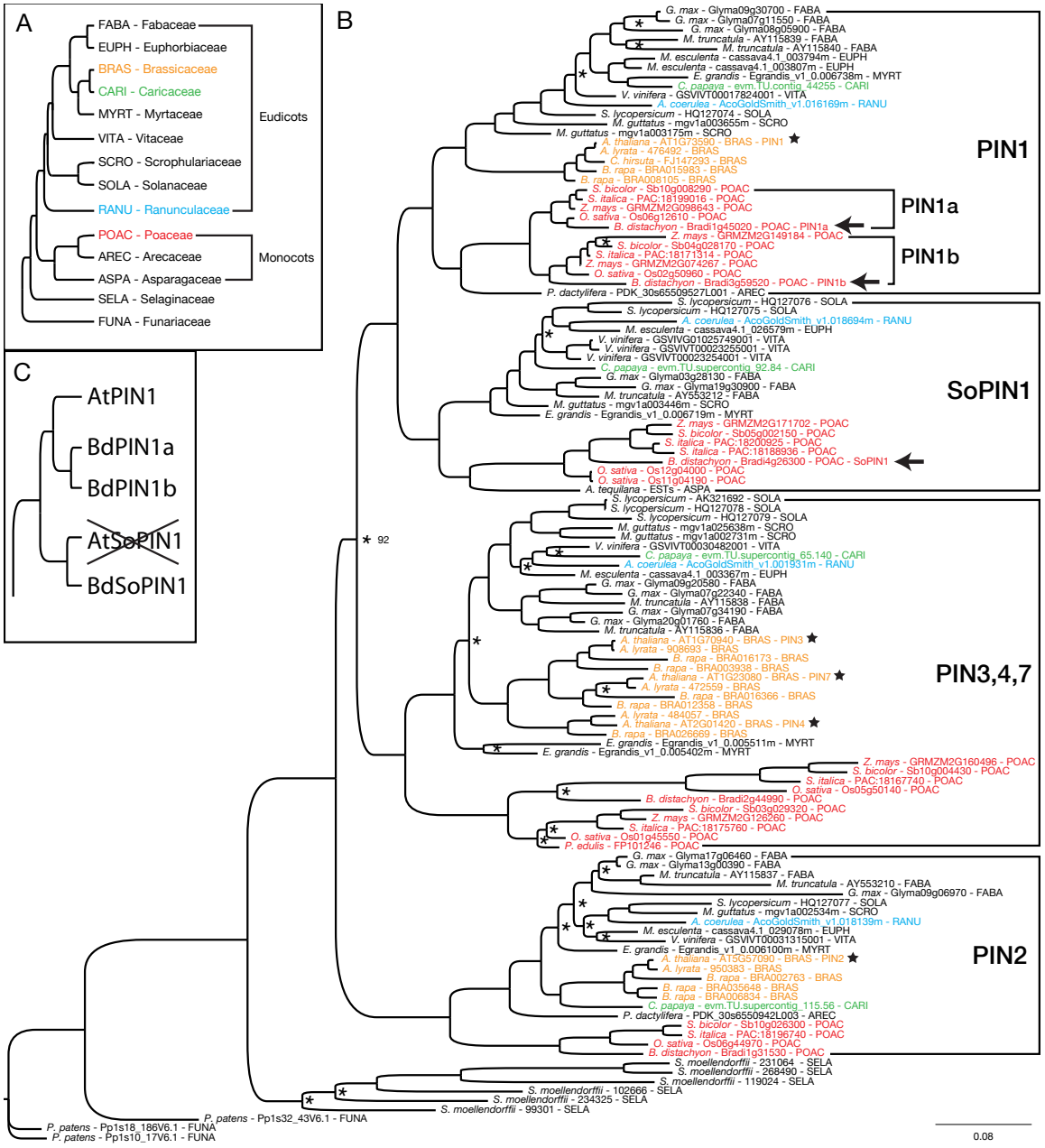

Figure 1

Figure 1: The Angiosperm Long-PINs. (A) Summary tree showing the relationships amongst the families sampled in B (Bremer et al. 2009). Families at major nodes are colored for clarity. Family abbreviations used in B preceded the family name. (B) Bayesian phylogram of angiosperm *Long-PIN* sequences. All nodes except those labeled with an asterisks (*) have at least 95% posterior probability. *Arabidopsis Long-PIN* sequences are marked with stars. Sequences of *Brachypodium SoPIN1*, *PIN1a*, and *PIN1b* are marked with arrows. Major

Long-PIN clades are labeled at right according to the closest *Arabidopsis* homolog with the exception of *SoPIN1*. Plant families at major phylogenetic nodes are colored according to A. Each sequence name is followed by a family abbreviation also defined in A. (C) Summary of inferred phylogenetic relationships between *Arabidopsis PIN1* and *Brachypodium SoPIN1*, *PIN1a*, and *PIN1b*. The “X” indicates loss of SoPIN1 in *Arabidopsis*.

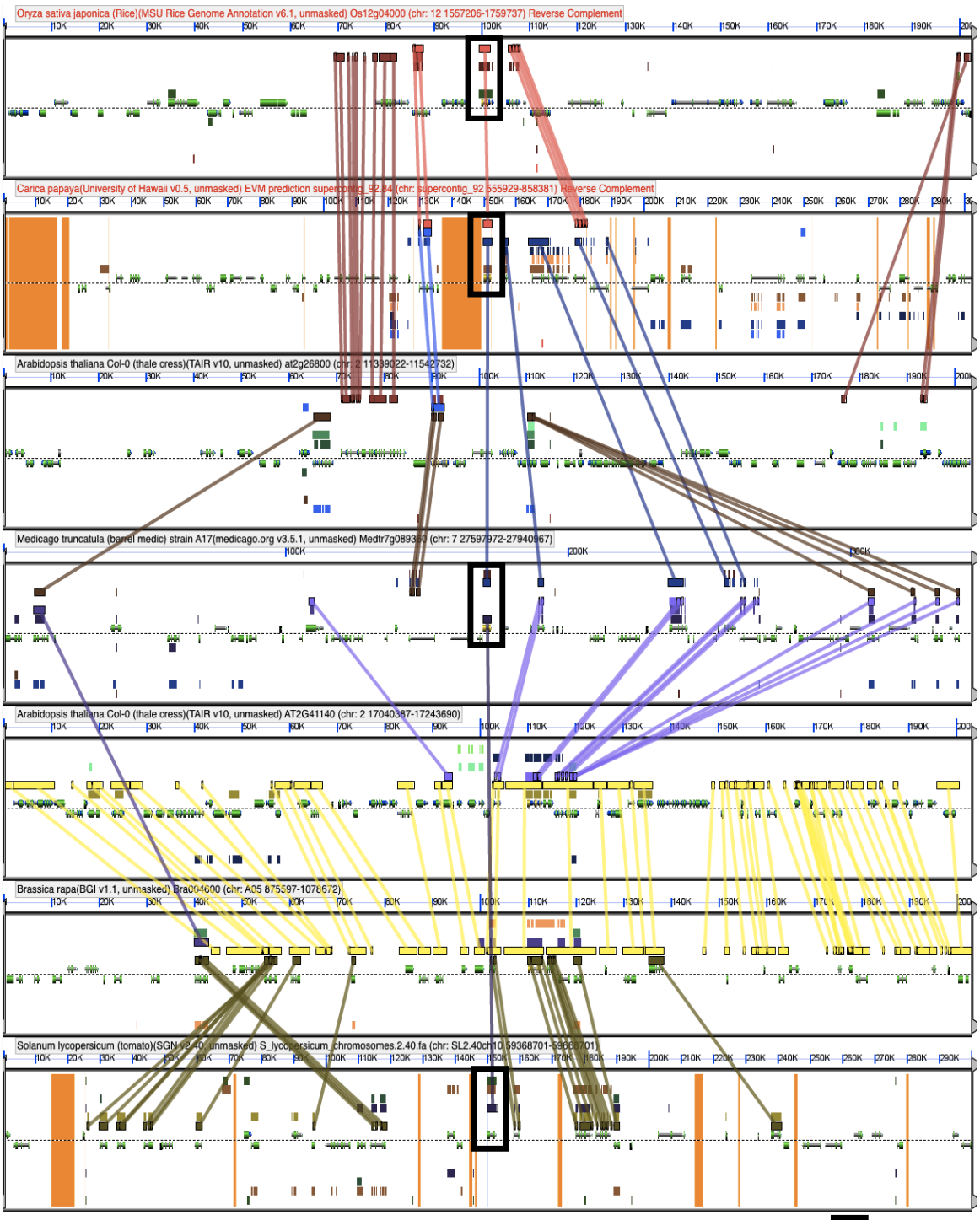

Figure 2: SoPIN1 is not present in the syntenic chromosomes of the *Brassicaceae*. CoGe analysis of syntenic chromosomes from *Oryza sativa*, *Papaya*, *Arabidopsis* thaliana (duplication *alpha* in upper track and *beta* in lower track), *Medicago*, *Brassica rapa*, and *Solanum lycopersicum*. Each row shows a syntenic chromosome from each organism. Gene models are blue and green and

are centered vertically on each track. Black boxes outline *SoPIN1* orthologs in species where *SoPIN1* has not been lost. Colored blocks above and below gene models are BLAST high scoring pairs (HSPs) between different organisms and are connected by colored lines. Synteny is partially preserved and several genes adjacent to *SoPIN1* are syntenous across all samples. However, *SoPIN1* is not present in any *Brassicaceae* species sampled.

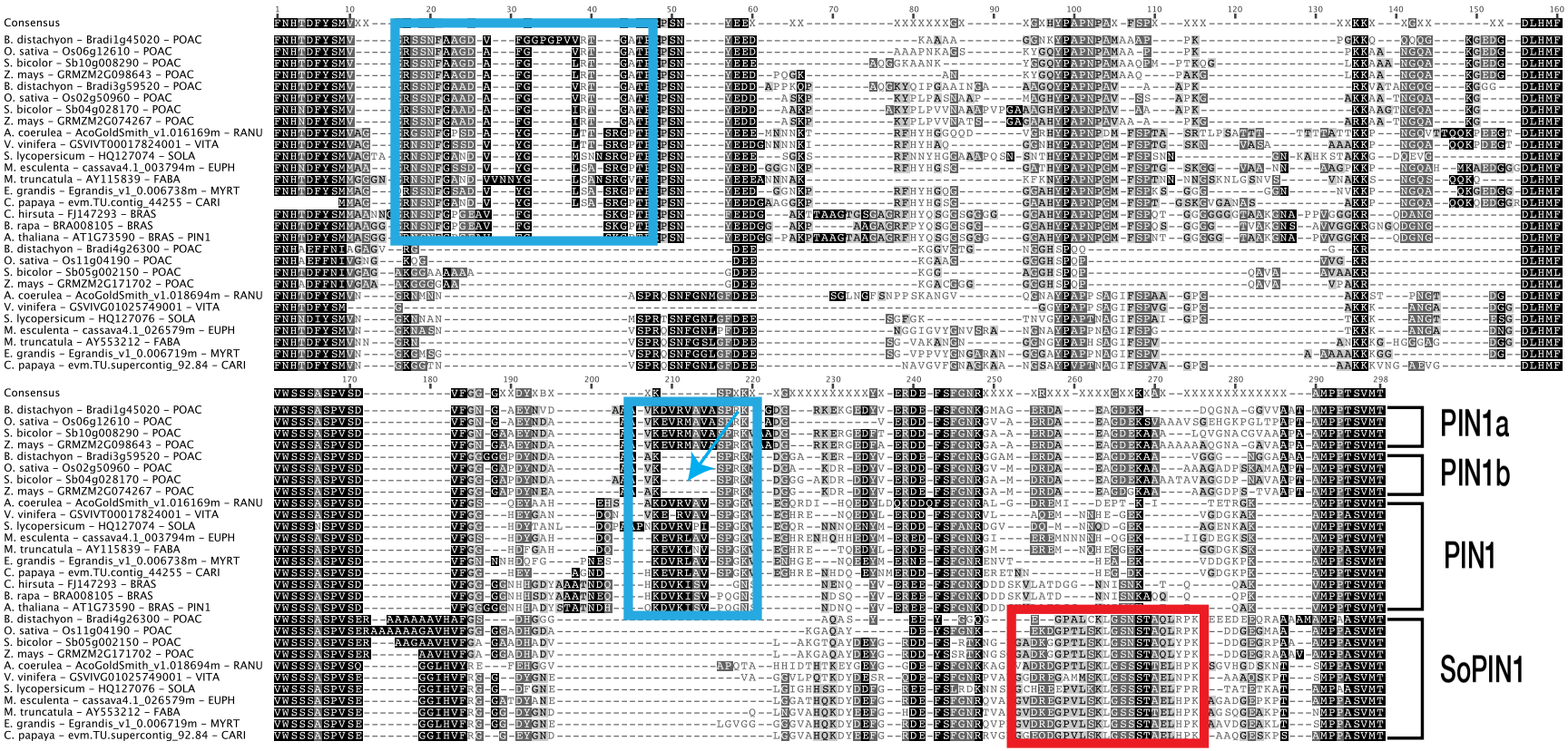

Figure 3

Figure 3: PIN1 and SoPIN1 proteins have different conserved domains in the hydrophilic region. Protein alignment of a portion of the variable hydrophilic domain of select PIN1a, PIN1b, PIN1 and SoPIN1 proteins. Clades are labeled at the end of the alignment. Amino acids are colored according to similarity. Blue rectangles indicate domains that are conserved in PIN1, PIN1a and PIN1b proteins that are absent in SoPIN1 proteins. The red rectangle indicates a SoPIN1 specific domain. The blue arrow shows a region within a PIN1 conserved domain that is deleted in PIN1b members. Over their entire length *Brachypodium* PIN1a and PIN1b have 81% identity. Whereas *Brachypodium* SoPIN1 has 58.9% identity with PIN1b and 61.1% identity with PIN1a.

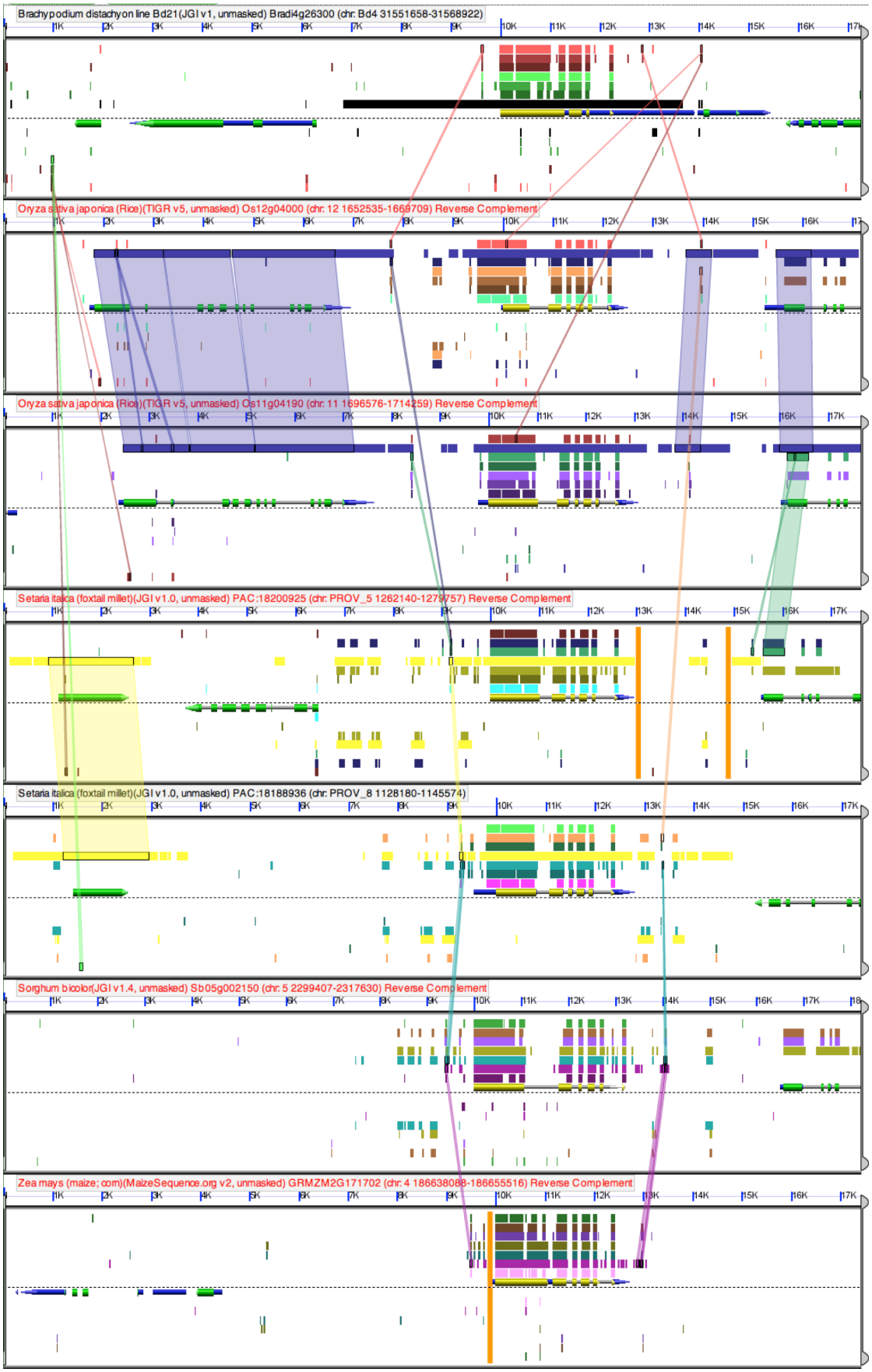
Brachypodium distachyon line Bd21(JGI v1, unmasked) Bradi4g26300 (chr: Bd4 31551658-31568922)
Oryza sativa japonica (Rice)(TIGR v5, unmasked) Os12g04000 (chr: 12 1652535-1669709) Reverse Complement
Oryza sativa japonica (Rice)(TIGR v5, unmasked) Os11g04190 (chr: 11 1696576-1714259) Reverse Complement
Setaria italica (foxtail millet)(JGI v1.0, unmasked) PAC:18200925 (chr: PROV_5 1262140-1279757) Reverse Complement
Setaria italica (foxtail millet)(JGI v1.0, unmasked) PAC:18188936 (chr: PROV_8 1128180-1145574)
Sorghum bicolor(JGI v1.4, unmasked) Sb05g002150 (chr: 5 2299407-2317630) Reverse Complement
Zea mays (maize; corn)(MaizeSequence.org v2, unmasked) GRMZM2G171702 (chr: 4 186638088-186655516) Reverse Complement

Figure 4: SoPIN1 CNS analysis across the grasses. Each row shows a syntenic chromosome from each organism. Exons in gene models for all syntenic *SoPIN1* orthologs are colored yellow, other exons in gene models in the syntenic region are colored green. Colored blocks along the chromosome are BlastN HSPs. HSPs that were visually identified to be conserved across most grass species are connected with lines and represent putative CNSs. The black bar in the *Brachypodium* track represents the region that was cloned for the florescent reporter construct (See Chapter 2).

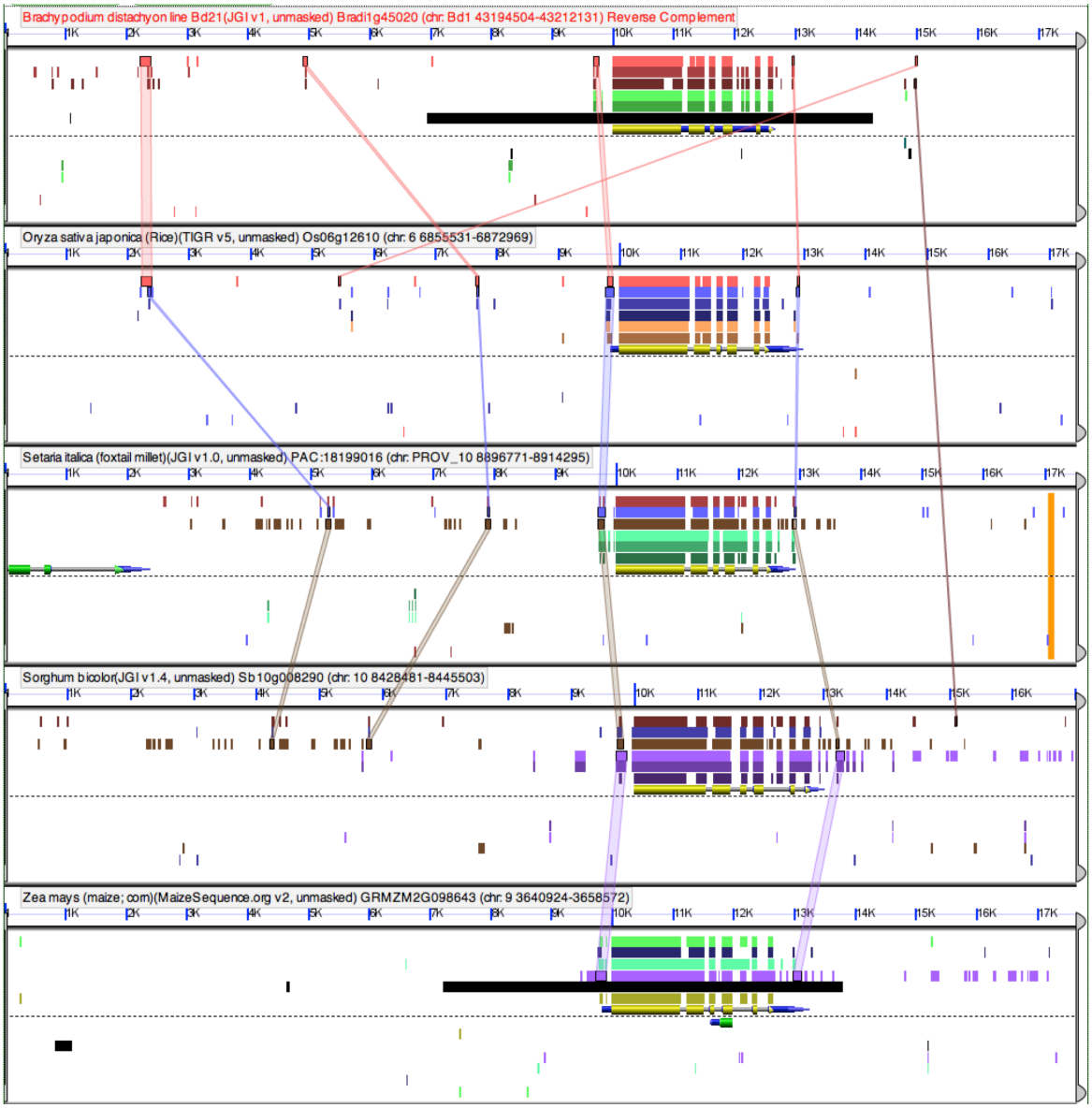

Figure 5: PIN1a CNS Analysis across the grasses. Each row shows a syntenic chromosome from each organism. Exons in gene models for all syntenic *PIN1a* orthologs are colored yellow, other exons in gene models in the syntenic region are colored green. Colored blocks along the chromosome are BLAST HSPs. HSPs that were visually identified to be conserved across most grass species are connected with lines and represent putative CNSs. The black bar in the *Brachypodium* track represents the region that was cloned for the *PIN1a* florescent reporter construct (See Chapter 2).

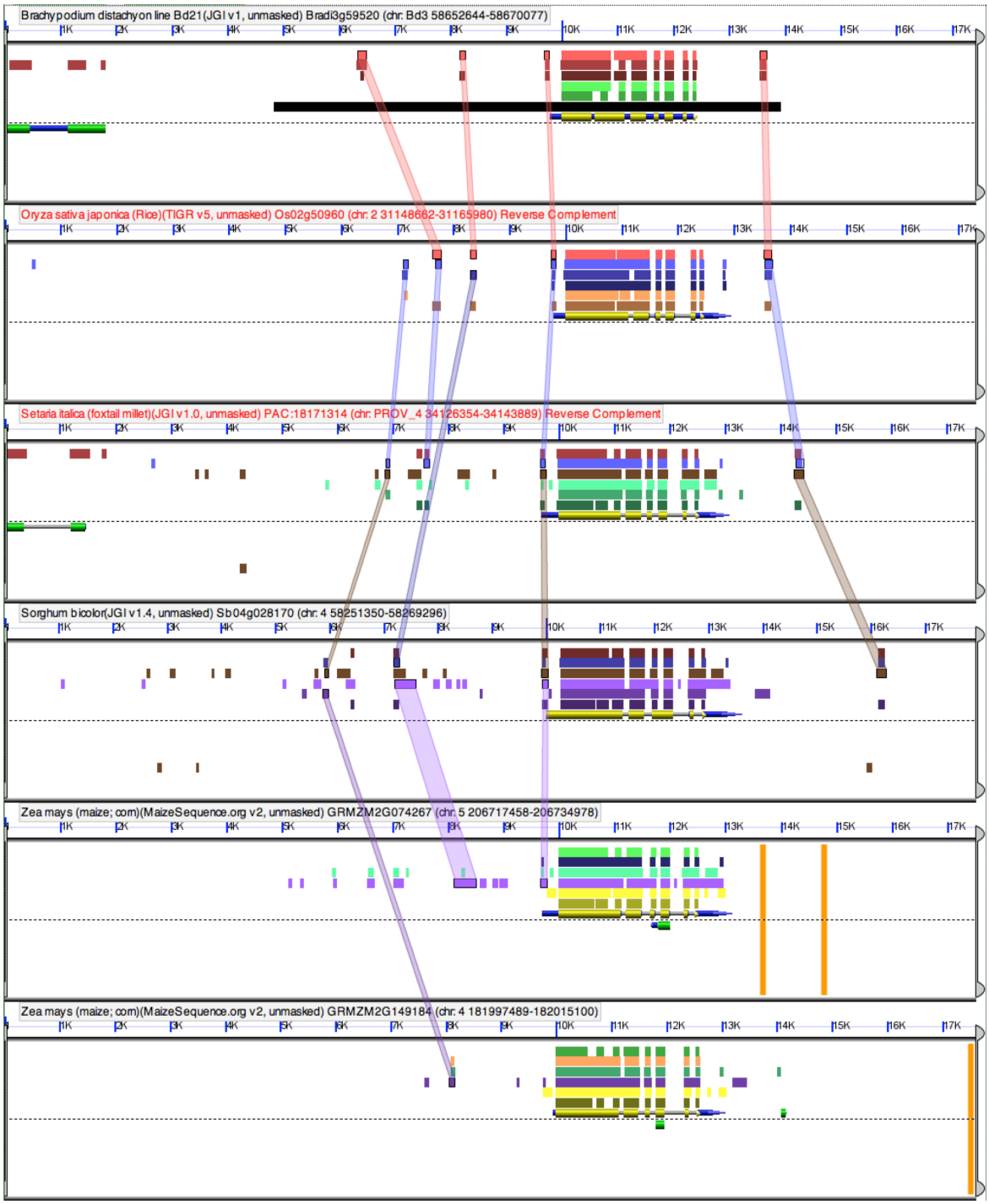

Figure 6: PIN1b CNS Analysis across the grasses. Each row shows a syntenic chromosome from each organism. Exons in gene models for all syntenic *PIN1b* orthologs are colored yellow, other exons in gene models in the syntenic region are colored green. Colored blocks along the chromosome are BLAST HSPs. HSPs that were visually identified to be conserved across most grass species are connected with lines and represent putative CNSs. The black bar in

the *Brachypodium* track represents the region that was cloned for the *PIN1b* florescent reporter construct (See Chapter 2).

Chapter 2: PIN Expression and Localization During *Brachypodium* Floral Development

Introduction

In order to explore the evolutionary and functional significance of the loss of SoPIN1 in the *Brassicaceae* and the duplication of PIN1 into PIN1a and PIN1b in the grasses I examined the expression and localization of PIN1a, PIN1b and SoPIN1 during *Brachypodium* spikelet development. The spikelet is the basic floral unit of the grasses and is composed of two sterile leaf-like bracts followed by florets in a distichous phyllotaxy (Figure 1: A, B). In *Brachypodium*, the inflorescence meristem initiates 0–4 lateral spikelet meristems in a distichous phyllotaxy before initiating the terminal spikelet meristem. Each *Brachypodium* spikelet meristem is indeterminate and initiates 2 sterile bracts followed by 7–14 floral meristems in a distichous phyllotaxy before terminating (Figure 1: B). The first product of each floral meristem is the lemma, a leaf-like organ that surrounds the remaining floral organs.

To visualize each PIN, I created stable transgenic plants containing full-length florescent-protein fusion constructs for *Brachypodium SoPIN1*, *PIN1a*, and *PIN1b* under their native promoters. In an effort to include all important regulatory sequences, the promoter and downstream regions were adjusted to include the majority of conserved non-coding sequences (CNS) identified in the syntenic genes across the grasses (Chapter 1, Figures 4-6). I first examined PIN expression and localization during lemma initiation. This stage had several advantages for live imaging; the spikelet meristem is relatively exposed, and the indeterminate nature of the *Brachypodium* spikelet meristem allows visualization of a developmental series of one leaf initiation event (lemma) and one axillary branch initiation event (floral meristem) at each node in a distichous phyllotaxy (Figure 1: A).

Results

Combined expression of SoPIN1, PIN1a, and PIN1b create the auxin transport path in the *Brachypodium* spikelet meristem.

SoPIN1, PIN1a, and PIN1b have partially overlapping but unique expression domains in the spikelet meristem. SoPIN1 expression is highest in the epidermal cell layer (Figure 1: C) and is reduced internally, especially in non-meristematic tissues (Figure 1: D). Significant internal expression of SoPIN1 is restricted to the sites of initiating organs and lateral veins (Figure 1: D). In contrast, PIN1a and PIN1b are almost exclusively expressed internally, at this stage primarily along the presumed paths of incipient lemma veins (Figure 1: E, F). In the epidermis, PIN1a and PIN1b are only expressed transiently in a few cells at the distal tips of both the midvein and lateral veins in P1 and older leaves (Figure 1: E, F). All three PINs partially overlap in incipient organs, but SoPIN1 dominates the

epidermis and PIN1b is expressed in the center of the developing spikelet and in the center of both the spikelet and floral meristems.

In order to visualize the entire potential path of auxin transport in the *Brachypodium* spikelet, I examined expression of the synthetic auxin signaling reporter DR5 driving an endoplasmic reticulum localized monomeric RFP (Gallavotti et al. 2008). DR5 expression is high in the epidermis of the apical dome, at the site of each lemma primordium, along the path of each incipient vein, and in a broad column down the center of the spikelet (Figure 1: G). Each of the three PINs is co-expressed with DR5 along a limited part of the entire DR5 domain (Figure 1: H for PIN1a) but only combined SoPIN1, PIN1a, and PIN1b expression matches the entire DR5 expression pattern in the *Brachypodium* spikelet. These data suggest that all three PINs likely act in concert to create the auxin transport path in the *Brachypodium* spikelet but that each PIN may have unique functions.

SoPIN1 creates convergence points

Detailed analysis of SoPIN1 cellular localization during lemma initiation identified two primordia at stages prior to morphogenesis, numbered here I2 and I1 in order of their appearance (I2, I1 in Figure 1: A Box). In the youngest incipient primordia, I2, localization of SoPIN1 in the epidermis is primarily oriented shootward, towards the meristem apex, while SoPIN1 localization at the apex of the spikelet meristem is oriented convergent, toward the side where the I2 primordia will eventually form (Figure 2: B, Red Arrows). At this stage, expression is mainly restricted to the epidermal cell layer and is relatively low. In I2 DR5 expression overlaps with SoPIN1 and is highest in the epidermis of the spikelet meristem apex with limited expression internally (Figure 2: A).

By I1, SoPIN1 expression increases and shows strong convergent localization, with shootward polarity in abaxial cells and rootward polarity in adaxial cells (Figure 2: A, B. Convergence point marked with asterisk). Sub-epidermal expression of SoPIN1 also increases in I1 and is convergent. In the sub-epidermal layers, SoPIN1 orients toward the epidermal convergence point in cells closest to the epidermis and convergent along the incipient midvein axis in more internal cells (Figure 2: B). SoPIN1 convergence in I1 is coincident with an increase in DR5 in the meristem epidermis as well as internally, suggesting an increase in auxin concentration around the I1 convergence point (Figure 2: A, C). Convergent polarization of SoPIN1 in I2 and I1 precedes lemma morphogenesis and predicts the location of the incipient midvein. In later stage I1 primordia, SoPIN1 convergence surrounds periclinal cell divisions, a hallmark of the beginning of leaf morphogenesis (Figure 2: B, Inset).

After primordia initiate, they are designated P1, P2, P3, etc., P1 being the most recently initiated and P3 being the oldest primordia. In P1 primordia SoPIN1 expression narrows at the tip of the incipient midvein and is highest in the

epidermal cells adjacent to the midvein convergence point (Figure 2: D). DR5 expression is maximal in these few epidermal cells as well (Figure 2: A). As the primordium expands, SoPIN1 expression is persists at low levels along the axis of the midvein oriented either toward the DR5 maxima at the leaf tip or parallel to the midvein axis (Figure 2: D). Also at P1, SoPIN1 expression increases at two secondary epidermal convergence points around the circumference of the meristem, coincident with the initiation of two secondary lemma veins (Figure 1: C circles). After the formation of convergence points during lemma midvein and lateral vein formation, SoPIN1 expression decreases dramatically at each convergence point, and by P3 expression at the midvein tip is almost gone (Figure 1: D).

In summary, SoPIN1 localization during lemma initiation is consistently oriented towards the presumed auxin maxima. Prior to the formation of I1 SoPIN1 is primarily oriented toward the DR5 maxima at the meristem apex; during I1 formation SoPIN1 is convergently localized toward the DR5 maxima at the site of the incipient midvein; and even in older P1 traces SoPIN1 is often oriented against the axis of the main midvein trace towards the epidermal midvein convergence point. Combined, these data suggest that SoPIN1 function during spikelet development is primarily the creation of auxin maxima at epidermal convergence points.

PIN1a and PIN1b canalize auxin transport

During lemma initiation, PIN1b is initially broadly expressed in the center of the meristem but is separated from the epidermis by at least 1 cell layer (Figure 2: F). At this stage, cellular polarity is often unclear and expression is relatively low. However, the domain of PIN1b in the apical dome is always connected to the PIN1b expression domain of the previous lemma midvein (Figure 1: F). At later stages, presumably after the creation of a convergence point maxima by SoPIN1, PIN1b expression in the apical dome becomes narrower, more lateral, and is continuous between the I1 epidermis and the PIN1b domain in the midvein of P1, loosely predicting the path of the I1 midvein (Figure 2: G). The PIN1b trace from I1 to P1 at this stage has more cells that show a clear polar localization directed diagonally across the spikelet meristem and connecting to the P1 midvein (Arrows Figure 2: G). At this stage DR5 expression increases across the SAM in the path of the I1 midvein (Figure 2: J-L).

By P1 PIN1b expression increases, and polarity is more ordered and contiguous, creating a distinct trace from the epidermis of P1 to the midvein of P2 (Figure 1: F). While expression is usually broad in P1, the inner two cell layers of the trace show the highest expression and a clear cellular polarization directed both rootward along the midvein path and inward towards the trace axis (Figure 2: G). PIN1b expression is highest in P1 and P2 primordia and decreases by P3 but is continuous between all primordia imaged at the stages examined (Figure 1: F).

Each midvein trace of PIN1b is connected by a central column of expression where polarity, when resolved, was rootward.

Expression of PIN1a occurs even later than SoPIN1 or PIN1b during lemma development. Expression is absent from the apical dome and is only present in a few cells of I1 (Figure 2: H). Sometimes the polarity of these cells is already oriented rootward and diagonal along the presumptive midvein path (Figure 2: H). Later, PIN1a expression along the P1 trace extends internally along the path of the midvein but remains only 1–2 cells wide. Polarity is consistently rootward and diagonal along the midvein trace (Figure 2: H). Remarkably, the PIN1a trace in P1 usually spans a region of low DR5 expression between the central column of DR5 and the maxima in the epidermis (Arrow in Figure 2: I, Figure 2: E). After spanning this gap in DR5 expression, the midvein PIN1a trace consistently terminates at the column of high DR5 and PIN1b expression in the center of the spikelet (Figure 1: E). Similar to PIN1a, high PIN1b expression is also associated with regions of lowered DR5 expression along vein traces (Figure 2: J-L) suggesting that both PIN1a and PIN1b may drain the trace of auxin when highly expressed.

In summary, the combined expression of PIN1a and PIN1b display many aspects of canalization. Both show minimal expression during the creation of epidermal convergence points, but rather their internal expression follows traces away from epidermal maxima. Expression of PIN1b is initially broad then narrows to roughly follow incipient midvein traces. Cellular localization begins relatively unordered and tissue polarity is unclear, but as development proceeds, localization becomes more polarized along presumptive midvein traces. PIN1b alone connects newly forming organs with the rest of the auxin transport path in older parts of the plant, yet does not canalize into as narrow a trace as PIN1a. Late PIN1a expression in a narrow file of polarized cells closely follows the presumed final vascular trace in each new primordia. This pattern suggests a degree of specialization between PIN1a and PIN1b, with PIN1b involved in the earlier stages of canalization and PIN1a defining the final canalized state.

Separation in PIN function is conserved in maize floral development

In order to validate these localization patterns from *Brachypodium,* polyclonal antibodies were raised to the maize SoPIN1, PIN1a, PIN1b, and PIN1c hydrophilic domains, similar to previously reported *A. thaliana* antibodies (Abas et al. 2006; Friml et al. 2002; Friml, Wisniewska et al. 2002; Friml et al. 2002; Gälweiler et al. 1998; Müller et al. 1998). Because of the high sequence similarity between PIN1a, PIN1b and PIN1c in this region in maize (64.7% pairwise identity), I was unable to entirely limit cross-reactivity between antibodies raised to these proteins. However, because SoPIN1 varies significantly in this region from members of the PIN1 clade, SoPIN1 immuno-localization on maize floral apices closely resembled the SoPIN1 domain found in *Brachypodium* (Figure 3: A). When localized in adjacent sections and staged meristems, a clear distinction

was observed between the primarily epidermal convergence of SoPIN1 (Figure 3: A, compare to Figure 2: B) and the canalization of PIN1a/b/c internally (Figure 3: B, compare to Figure 2: G). These results both validate my reporters as well as suggest that the functional division between SoPIN1 and PIN1 proteins is conserved at least across the grasses.

SoPIN1 and PIN1a show a similar functional division during vein canalization

Leaf veins in *Brachypodium* remain largely parallel for most of their length (Figure 4: A). During vein development, most new parallel PIN traces form de-novo between existing vein traces, allowing me to examine how SoPIN1, PIN1a and PIN1b interact during isolated canalization events (Figure 4: D). SoPIN1 expression in leaves is highest in the abaxial epidermis along the length of each nascent vein trace, but extends internally in a triangular shape towards where the vascular trace will form (Figure 4: B, Arrow). SoPIN1 expression in older traces decreases in the abaxial epidermis and becomes more radial (Figure 4: B, Circle). When colocalized with DR5, a clear line of epidermal SoPIN1 expression was observed along each nascent vein trace prior to significant expression of DR5, again suggesting that SoPIN1 precedes the formation of auxin maxima (Figure 4: D Arrow).

In order to examine how SoPIN1 relates to the expression of PIN1a, which is highly expressed in leaf vein traces, I created transgenic plants co-expressing Citrine and TagRFP-T fused versions of both proteins. Unfortunately, when either protein was tagged with TagRFP-T, the cellular localization of PIN was altered, making analysis of cell polarity impossible (Figure 4: C and E). However when compared to the Citrine tagged versions, I believe that the TagRFP-T versions accurately portray the expression domain of each protein. When colocalized, I observed that SoPIN1 expression precedes expression of PIN1a in each nascent vein trace (Figure 4: E Arrow). Once PIN1a expression increases in older traces, SoPIN1 expression remains in a broader domain, surrounding the canalized PIN1a trace (Figure 4: C). Thus, similar to organ initiation, expression of SoPIN1 during vein canalization precedes maxima creation, as assayed by the expression of DR5, as well as canalization, as assayed by PIN1a expression.

Discussion

Functional division of Up-the-Gradient and With-the-Flux auxin transport

Computational models of auxin patterning in the shoot focus on positive feedback regulation of auxin transport in response to auxin concentration (Garnett et al. 2010). Models based on the work of Sachs (Sachs 1981; 1969) proposed that within each cell, auxin transport is facilitated in the direction of the highest auxin flux (Mitchison 1981; 1980). Simulations of this “with-the-flux” type of transport

regulation can accurately recapitulate the formation of canalized traces and have been useful in explaining how PIN1 mediates vein development.

Complimentary models, primarily relating to how convergent localization of PIN1 facilitates the formation of auxin maxima in the meristem epidermis, propose an alternate positive feedback regulation where in each cell PIN1 is allocated to the cell membrane adjacent to the neighboring cell with the highest auxin concentration (Jönsson et al. 2006; R S Smith 2006). The result is the movement of auxin against the concentration gradient. Such "up-the-gradient" models are able to accurately recapitulate the initial steps of organ initiation, the formation of PIN1 convergence points and auxin maxima in the correct phyllotactic patterns, but are difficult to reconcile with experimental evidence showing PIN1 oriented rootward toward areas of low auxin concentration during the canalization of the midvein. In the unified model of Bayer et al, PIN1 dynamically switches between two functional modes depending on the auxin concentration, acting primarily up-the-gradient during the formation of auxin maxima, and with-the-flux once a threshold auxin concentration is reached during the canalization of the midvein (Bayer et al. 2009).

My characterization of SoPIN1, PIN1a, and PIN1b in *Brachypodium* support the functional division of PIN action into up-the-gradient and with-the-flux modes. Expression of SoPIN1 at sites of leaf and vein initiation and cellular localization of SoPIN1 oriented toward the presumed auxin maximum, is consistent with up-the-gradient transport. In contrast, PIN1a and PIN1b are consistently oriented away from auxin maxima, are initially broadly expressed, and then narrow into presumptive vein traces, characteristics of with-the-flux canalization. The division of up-the-gradient and with-the-flux functions between several different PIN proteins in *Brachypodium* both validates existing models and suggests that in other species transport routes presumed to be mediated mostly by PIN1 may be mediated by several different proteins.

The initial with-the-flux canalization models predicted a lower auxin concentration in canalized traces compared to the surrounding tissue (Mitchison 1981; 1980). Similar to *Arabidopsis*, my results somewhat contradict these models, and canalization of both PIN1a and PIN1b overlap with high DR5, indicating high auxin concentration within high flux traces (Figure 1). However, I observed that in many cases, the region along each trace axis with the highest PIN1a or PIN1b expression correlated precisely with an area of reduced DR5 expression, suggesting that high flux can transiently reduce the auxin concentration within a canalized trace (Figure 2 H-L). To account for the high auxin concentration observed within high flux traces, subsequent canalization models proposed the existence of up-the-gradient auxin transport surrounding the high flux trace (Bayer et al. 2009; Kramer 2004). My results show SoPIN1 oriented toward the axis of incipient lemma midveins, where DR5 is high, suggesting that SoPIN1 fulfills this function (Figure 2: B, C). Also, during leaf vein initiation, SoPIN1 expression was detected surrounding each PIN1a vein trace, suggesting that

SoPIN1 may continue to stabilize canalization events later in leaf development (Figure 4: C). These results are similar to localization studies in tomato and *Arabidopsis* that show PIN1 oriented toward the center of older vein traces (Bayer et al. 2009; Reinhardt et al. 2003). Thus my results support the idea that with-the-flux transport can drain a trace of auxin, but that up-the-gradient transport surrounding the trace may act to keep the concentration high despite high flux.

PIN1b expression suggests a greater role for sink

One problem with the dual function model is the inability of simulations to consistently predict where canalized traces will terminate, which is highly ordered during plant development (Bayer et al. 2009). For example, in tomato the canalization path of I1 invariably connects with the midvein of P3. The consistency of this connection lead the authors in Bayer et. al. to infer the possible existence of a diffusible signal derived from older veins that directs new canalization events. In support of this idea the authors were able to redirect canalization of I1 to the P2 midvein by surgically removing the P3 midvein (Bayer et al. 2009). An alternate hypothesis is that auxin transport is at least partially mediated by other broadly expressed and as yet uncharacterized transporters, or PIN1 below the level of detection. If this is the case then transport would be continuous between existing veins and the sites of newly initiating canalization events. The result is that canalization routes are to a degree pre-patterned before maxima formation (Kramer 2004). My analysis of PIN1b supports this latter idea. In the spikelet PIN1b is initially broadly expressed and centralized, but presumably after convergence point formation becomes more canalized, while at the same time connecting any new canalization events to earlier leaf traces (Figure 2; F, G). I propose that PIN1b initially acts as a less canalized ambiguous sink by connecting most cells in the meristem to the remainder of the auxin transport path in older tissues. In this way PIN1b pre-patterns the canalization path of the new leaf trace.

It follows that before maxima formation by SoPIN1 occurs, the un-canalized central domain of PIN1b may keep the auxin concentration low by shuttling auxin from the central meristem zone. Both modeling and experimental evidence suggests that PIN1 canalization may be induced at a threshold auxin concentration (Bayer et al. 2009; Heisler et al. 2005; Scarpella et al. 2006). Thus high levels of PIN1b may be dependent on a threshold auxin concentration, and thus dependent maxima formation by SoPIN1. To explain the delay in PIN1a expression, I further hypothesize that the threshold required for PIN1a expression is even higher than PIN1b, and thus PIN1b suppresses PIN1a canalization during the early stages of organ initiation by keeping the auxin concentration below threshold. As the auxin concentration reaches a threshold later in development, expression of PIN1a responds to the early gradient established by SoPIN1/PIN1b and helps canalize a more differentiated auxin transport path directly coupled with the patterning of the procambium.

In summary, my results support the idea that the creation of both an auxin source in the epidermis and a continuous connection to an auxin sink in the internal tissues is involved in leaf initiation and vascular patterning.

Loss of PIN functional division in the *Brassicaceae*

My phylogenetic analysis supports 4 major clades of Long-PIN proteins within the angiosperms, one of which, *SoPIN1*, was lost in the lineage leading to the *Brassicaceae*. Given that my results indicate a functional division between the *SoPIN1* and *PIN1* clades, the loss of *SoPIN1* within the *Brassicaceae* may indicate that *PIN1* in this group has acquired new functions, namely up-the-gradient transport. In addition, my analysis of SoPIN1, PIN1a and PIN1b localization in *Brachypodium* indicate that a functional division likely exists between SoPIN1 and PIN1 in other eudicots where SoPIN1 has not been lost.

So far, two different *Brassicaceae* species, *Arabidopsis thaliana* and *Cardamine hirsuta*, have described PIN1 mutants and both have similar mutant phenotypes. Most notably these mutants show an inability to initiate lateral organs and have naked, “pin-formed” inflorescence meristems (Gälweiler et al. 1998; Barkoulas et al. 2008). In addition, *A. thaliana pin1* mutants show a reduction in leaf serrations and in *C. hirsuta*, which has compound leaves, there is a reduction in leaf complexity, lateral leaflets are reduced or absent. Previous work has shown that the molecular program involved in the initiation of leaflets overlaps with the program for leaf serrations in simple leaved plants, and with leaf initiation itself (Barkoulas et al. 2008; Hay et al. 2006; Koenig et al. 2009; Barkoulas et al. 2008; Bilsborough et al. 2011; Hay et al. 2006; Hay and Tsiantis 2006; Koenig et al. 2009). Thus PIN1 mutants *Brassicaceae* species show similar defects in both the initiation and morphogenesis of lateral organs.

The first mutant in a member of the SoPIN1 clade was recently reported in another compound leaf eudicot species, *Medicago truncatula*, which has members of both the PIN1 and SoPIN1 clades (Chapter 1, Figure 1). Remarkably, in contrast to *A. thaliana* and *C. hirsuta pin1* mutants, *Medicago smooth leaf margin1* (*slm1*) mutants do not show a pin-formed phenotype and actually have an increased flower number in the inflorescence (Peng and Chen 2011). Similar to *C.hirsuta* mutants, *slm1* plants have fewer lateral leaflets, but unlike *C. hirsuta, slm1* mutants show an increase in the number of terminal leaflets (Peng and Chen 2011; Zhou et al. 2011). These phenotypes suggest a limited functional overlap between *Brassicaceae* PIN1 and SoPIN1/SLM1.

I hypothesize that the differences in phenotype between *C.hirsuta pin1* mutants and *Medicago slm1* mutants could be explained if in *Medicago* there exists a functional division between SoPIN1/SLM1 and PIN1 similar to *Brachypodium*, whereas in the *Brassicaceae* PIN1 performs both functions. Thus in *Medicago* and other species with both SoPIN1 and PIN1, mutations in both would be

required to fully perturb organ initiation, whereas this is not true for *A. thaliana* and *C. hirsuta*. Indeed expression of SLM1 by in-situ hybridization is primarily detected at the sites of initiating organs, consistent with a role in maxima formation similar to SoPIN1 in *Brachypodium*. In addition, DR5 expression is increased in the margin of *slm1* mutants, suggesting that without convergence mediated by SLM1/SoPIN1, auxin accumulates in the leaf margin (Zhou et al. 2011). If SLM1 in *Medicago* does function similar to SoPIN1 in *Brachypodium* then this suggests a greater role for internal canalization mediated by PIN1 during leaf initiation because leaf initiation is not aborted in *slm1* mutants as it is in *Brassicaceae pin1* mutants.

In conclusion, I propose that internal canalization of the auxin transport stream has an important role in defining the location of auxin gradients. Epidermal maxima likely serve as important organizing cues to trigger canalization at a particular point, but in the absence of such cues internal canalization can proceed, as is the case in *slm1* mutants. Alternatively, in the absence of SLM1/SoPIN1 other PIN proteins may become expressed and take over SoPIN1 function as has been described for *pin* mutants in *Arabidopsis* (Vieten et al. 2005; Paponov et al. 2005). Regardless, my results suggest that it is probably the relative contributions of cues from both internal canalization and epidermal maxima that define the overall shape and organization of leaf initiation and lamina development.

Materials and Methods

Reporter Constructs and plant transformation

Full-length PIN reporter constructs were cloned using a three fragment Multisite Gateway recombination system (Invitrogen). For each construct the promoter and the 5' part of the gene was cloned into pDONR-P4-P1R. For the 5' fragment, 3045, 5164, and 3147 nt of upstream sequence from the ATG, and 652, 652, and 709 nt of downstream sequence from the ATG was cloned for PIN1a, PIN1b, and SoPIN1 respectively. For the middle gateway fragment, the YFP variant Citrine and the mRFP variant TagRFP-T were cloned into pDONR221 with 5x Ala linkers. The start and stop codons were removed. The 3' end of each gene and downstream sequences were cloned into pDONR-P2R-P3. For the 3' fragment, in addition to the rest of the gene following the internal fusion, 1652, 1512, 1403 nt of downstream sequence from the stop codon was cloned for PIN1a, PIN1b, and SoPIN1 respectively. All three fragments were recombined into the Gateway binary vector pH7m34GW. The location of Citrine in the resulting internal protein fusions was in a homologous position to a previously characterized *Arabidopsis* PIN1::GFP fusion (Heisler et al. 2005) and a Citrine tagged PIN1a fusion in maize (Gallavotti et al. 2008). The DR5 construct was described previously (Gallavotti et al. 2008) and was transformed directly into *Brachypodium* unaltered. *Brachypodium* transformation was performed as described (Vogel et al. 2007) . At least 3 events were characterized for each PIN fusion construct

while only 2 events were recovered for DR5. However, both DR5 events showed identical expression in all tissues analyzed and expression was similar to results reported for maize (Gallavotti et al. 2008).

Immuno-localization

Vegetative shoot apexes were dissected and fixed overnight in FAA (Formaldehyde and Acetic Acid). After ethanol dehydration, samples were imbedded in Steedman's polyester wax. 9 µm sections were mounted, dewaxed in ethanol, dried, then rehydrated into PBS. Slides were blocked with 5% Donkey serum in PBS then probed. Antibody dilutions: 1:50 Rabbit anti GFP sc-8334 (Santa Cruz), 1:200 anti-SoPIN1, or 1:200 anti-PIN1a/b/c. After washing in 1% Fish Gelatin in PBS, slides were probed with 1:200 anti-rabbit cy3 conjugated florescent secondary (Jackson Immuno). Finally, slides were washed again and mounted with DABCO glycerol mounting media. Images were captured on a Zeiss AxioVert with 20x objective and processed using ImageJ.

Image Acquisition and Analysis

Florescent reporter lines were imaged using a Leica TCS SP5 laser scanning confocal. Tissue was mounted in water with or without a cover slip. Citrine was excited using the 514 laser line and mRFP using the 561 laser line. For all samples the pinhole was set to one Airy unit. A water dipping 20x objective, NA 0.7 was used. Gain offset, and z-stack settings were adjusted according to the tissue being imaged and the strength of expression. For all images, transmitted laser light was detected simultaneously to create bright-field images. Double DR5 and PIN::Citrine combinations were generated by crossing homozygous DR5 plants to heterozygous or homozygous PIN::Citrine plants. Images were captured in the F1 generation of this cross.

Images were processed using ImageJ. First, florescence channels were separated from the transmitted light channel. In most images, the transmitted light stack was reduced to a single plane using an extended depth of field plugin (http://bigwww.epfl.ch/demo/edf/). This plugin attempts to create a single in-focus image by removing out of focus information in each section of the stack. Florescent channels were processed with a median filter to reduce noise. In some images, individual florescent z-planes were recombined with the processed transmitted light images to create the final image. In other images, florescent stacks were reduced to maximum projections then combined with the processed transmitted light channel to create the final image. Florescent look-up-tables were used to show variation in florescent intensity with different colors (Figure 1B inset).

Figures

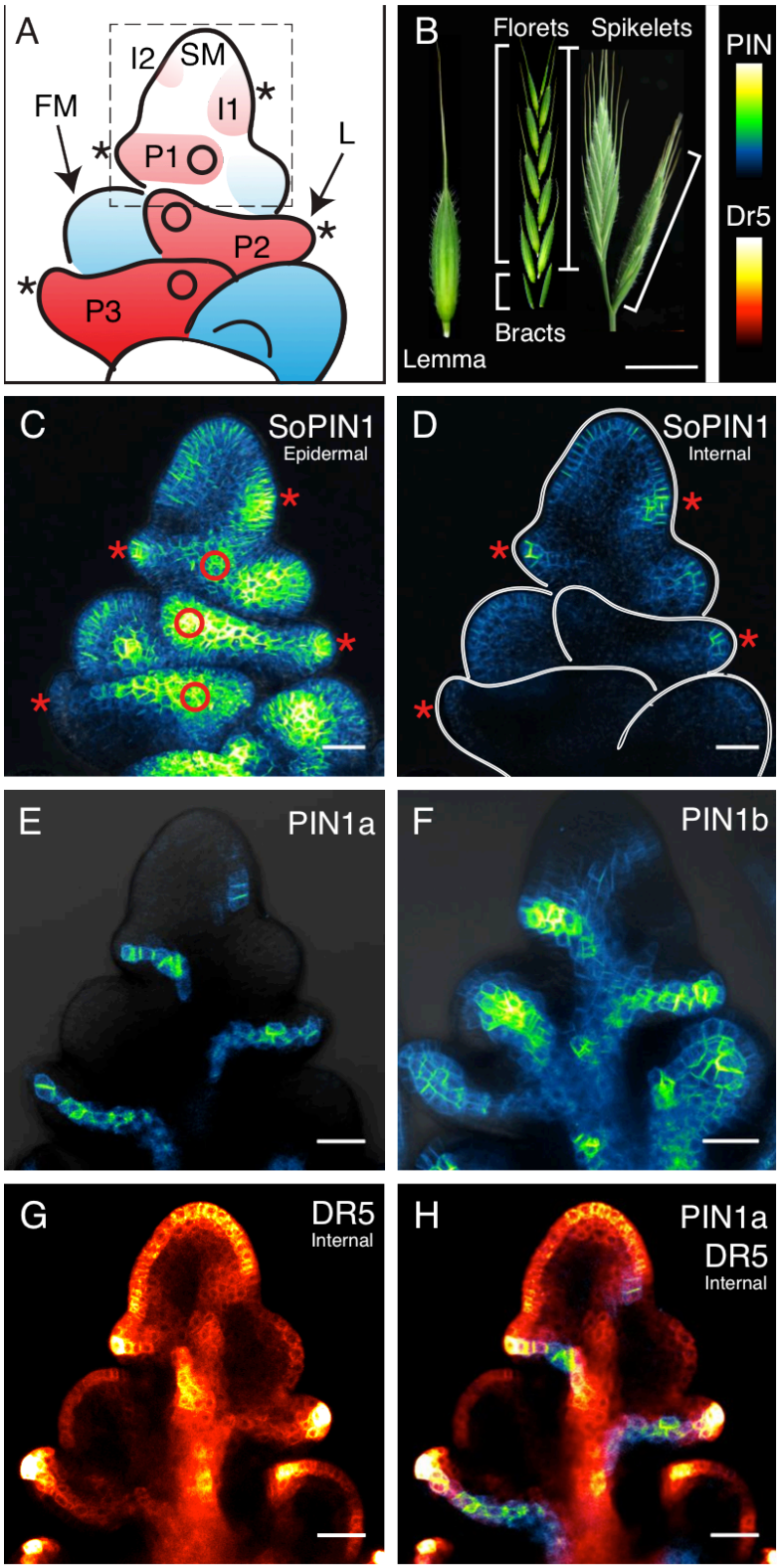

Figure 1

Figure 1: PIN Expression During Brachypodium Spikelet Development. (A) Illustration of the *Brachypodium* spikelet meristem. Lemma primordia are colored red, floral meristems colored blue. Lemma primordia are labeled in the order of emergence I2, I1, P1, P2, P3. The SM: Spikelet Meristem, and a single FM: Floral Meristem and L: Lemma primordium are labeled. Box indicates area of detail images in Figure 2. (B) The *Brachypodium* inflorescence (right) showing one lateral and one terminal spikelet. Middle shows a single spikelet broken into individual florets, and left shows a single floret lemma. (B Inset) Look-up-table scales for florescence images. (C-H) Confocal maximum projections of PIN and DR5 expression in staged *Brachypodium* spikelet meristems. (C,D) SoPIN1. (C) Maximum projection of SoPIN1 that includes epidermal confocal sections. (D) Only internal confocal sections of the same sample as (C). (E, G, H) PIN1a and DR5 from single PIN1a and DR5 expressing plant. (E) PIN1a channel only, (G) DR5 only, (H) DR5 and PIN1a. (F) PIN1b. Only internal DR5 sections are shown in (G-H). Asterisks in (A), (C), and (D) show lemma midvein convergence points. Circles in (A) and (C) show lemma lateral vein convergence points. Scale bars: 1cm in B, 25μm in C-H.

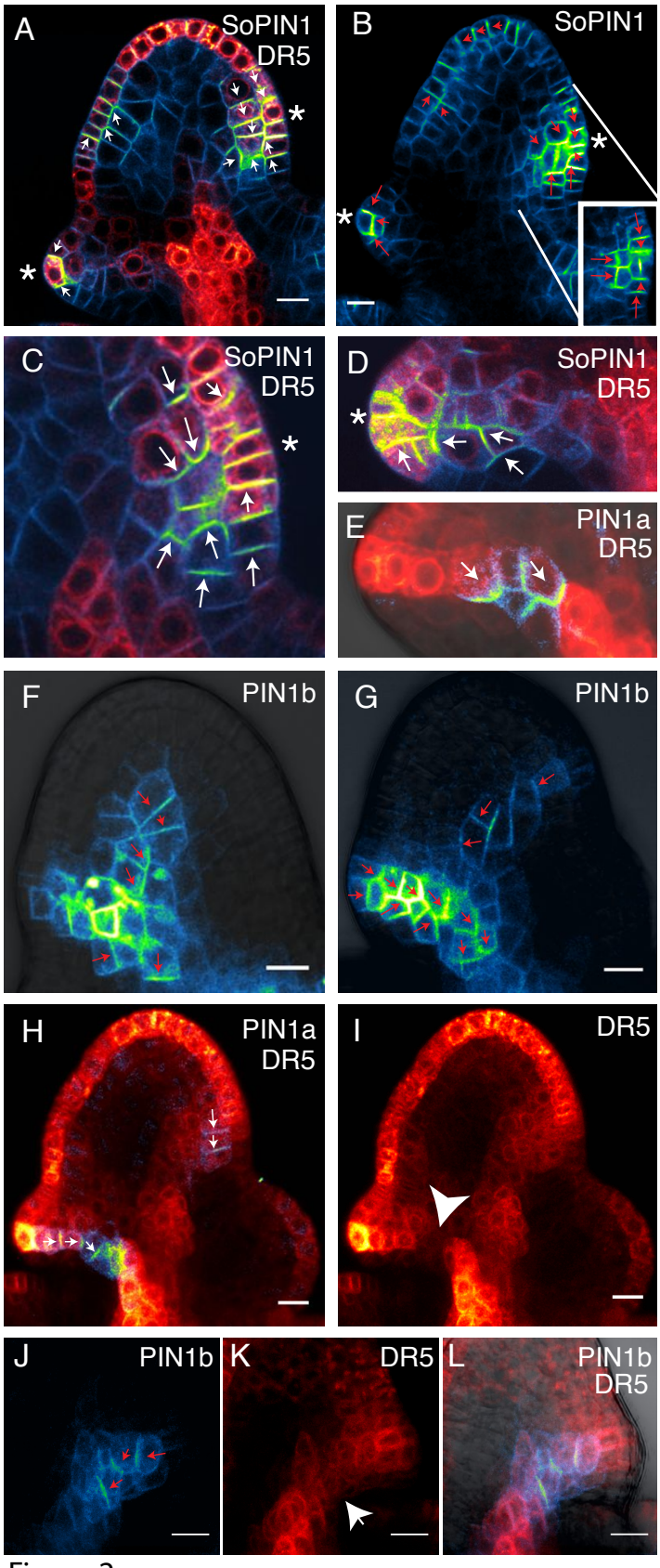
A
SoPIN1
DR5
B
SoPIN1
C
SoPIN1
DR5
D
SoPIN1
DR5
E
PIN1a
DR5
F
PIN1b
G
PIN1b
H
PIN1a
DR5
I
DR5
J
PIN1b
K
DR5
L
PIN1b
DR5

Figure 2

Figure 2: PIN Cellular Localization During Lemma Initiation. (B, G, H, I) Details of same samples as Figure 2: C-H. Detail area is indicated by the box in Figure 1: A. (A, C, D, E, F) Alternate samples of SoPIN1, PIN1a and PIN1b. (A) SoPIN1 and DR5 expression. (B) SoPIN1 expression at a later stage than (A). Inset shows alternate confocal section of same dataset with an epidermal periclinal cell division. (C) I1 detail of SoPIN1 and DR5. (D) Detail of SoPIN1 and DR5 in P1 midvein. (E) PIN1a and DR5 in P1 midvein. (F) PIN1b early stage. (G) PIN1b at later stage than (F). (H) PIN1a and DR5. (I) Same dataset as H, DR5 channel only. Arrow-head shows region of lowered DR5 expression along the P1 midvein spanned by PIN1a. (J-L) DR5 expression is reduced in areas of high PIN1b expression. (J) PIN1b, (K) DR5, and (L) merged images of a P1 lemma primordia. Note reduced DR5 in the PIN1b midvein domain. Asterisks show lemma convergence points in A-D. Arrows in A-J indicate inferred polarity of PIN. Scale Bars: 10μm.

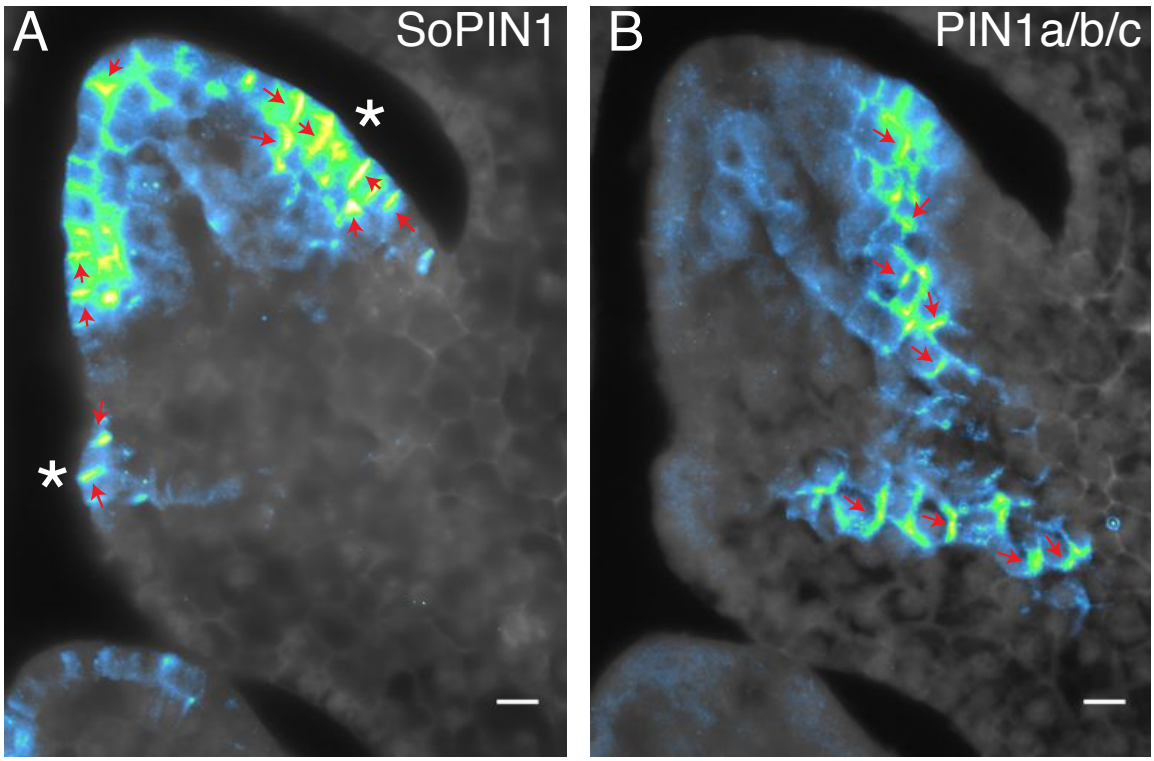

Figure 3

Figure 3: PIN localization in Maize Spikelet Meristems. (A) Anti-SoPIN1, (B) Anti-PIN1a/b/c immunolocalization in adjacent sections. Asterisk indicate midvein convergence points. Arrows indicate inferred polarity of PIN. Scale Bars: 25μm.

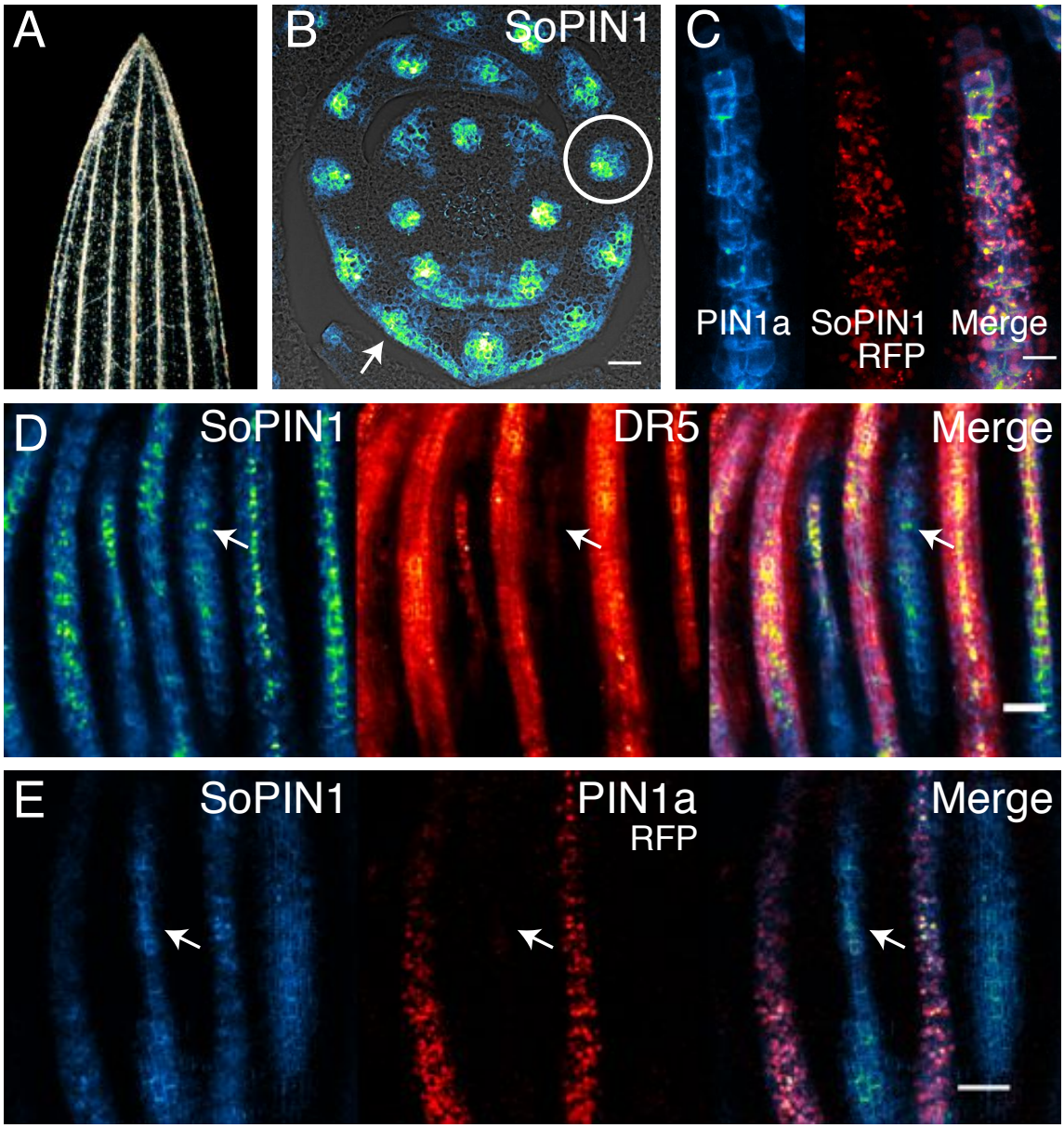

Figure 4

Figure 4: PIN Localization During the Canalization of Leaf Veins. (A) Cleared vegetative leaf showing parallel leaf veins. (B) Anti-GFP immunolocalization of Citrine tagged SoPIN1 in a cross section of the vegetative stem and leaf. Arrow indicates SoPIN1 expression in the abaxial epidermis in a new vein trace, while the circle indicates an older vein trace where SoPIN1 expression decreases in the epidermis. (C) Co-localization of PIN1a and SoPIN1 in a vegetative leaf vein trace. PIN1a::Citrine (left), SoPIN1::TagRFP-T (middle) and merge (right). (D) Colocalization of SoPIN1 and DR5 in vegetative leaf vein traces. SoPIN1 (left), DR5 (middle) and merge (right). (E) Co-localization of SoPIN1 and PIN1a in a vegetative leaf vein traces. SoPIN1::Citrine (left), PIN1a::TagRFP-T (middle) and

merge (right). Arrows indicate the same vein trace in (D) and in (E). Scale Bars: 50μm in B, 10μm in C and 25μm in D, E.

Chapter 3: PIN Expression and Localization During *Brachypodium* Vegetative Development

Introduction

Plants show dramatic variation in leaf morphology, vein patterning, and phyllotaxy. However, much of the work on PIN-mediated patterning has focused on shapes that are unique to only certain eudicot groups. In *Arabidopsis*, leaves are initiated in a whorled phyllotactic pattern and leaf veins are reticulate (Nelson and Dengler 1997; Tang et al. 2003). However, in many monocots such as grasses, leaves are initiated in a distichous phyllotactic pattern, with new leaves 180 degrees from older ones. In addition, monocots tend to have a stem anatomy with "scattered" vascular bundles, and a leaf venation pattern that is largely parallel (Sharman 1942). It is likely that because auxin transport is a common patterning mechanism it may have played a role in the evolution of these differences.

In my phylogenetic analysis, the lineage specific duplication in the PIN1 clade that gave rise to PIN1a and PIN1b is unique to the grasses sampled (Chapter 1 Figure 1B). While my sampling within the monocots was limited by the available genomes, I hypothesize that if this duplication is conserved within the monocots it may relate to the characteristic aspects of monocot leaf initiation and vein patterning. Thus I examined SoPIN1, PIN1a, and PIN1b expression during *Brachypodium* vegetative leaf development, where the encircling leaf base and parallel veins characteristic of monocot plants can be easily observed.

Results

A radial auxin maxima mediated by SoPIN1 proceeds Brachypodium vegetative leaf initiation

During vegetative leaf initiation in *Brachypodium*, primordia begin as a bulge at the site of the incipient midvein but later wrap almost entirely around the circumference of the stem, often enclosing the SAM and several younger leaf primordia under a hood of lamina tissue (Figure 1: A, F). In general, the expression and localization of SoPIN1, PIN1a and PIN1b during vegetative leaf initiation closely resembles lemma initiation; SoPIN1 is maximal in the epidermis and convergent at the site of the midvein; PIN1b is expressed in the center of the stem and connects each initiating leaf; and PIN1a is expressed at later stages in narrow files of cells along the presumptive paths of initiating veins (Figure 1: B, C, D). Thus SoPIN1, PIN1a, and PIN1b function similarly during vegetative and floral development.

However, during vegetative leaf initiation the formation of a radial epidermal auxin maxima mediated by SoPIN1 convergence was clearly observed. At I2 SoPIN1 shows convergent localization in the vegetative meristem epidermis at

the site of the presumptive midvein (Figure 2: A). When imaged in cross section, SoPIN1 convergence at I2 is initially broad and involves several cell layers (Figure 2: C). By I1, SoPIN1 forms a ring shape around the meristem circumference, with maximal expression in the epidermis at the midvein and strong expression continuing in a narrow epidermal ring around the circumference of the SAM (Figure 2: B, E). At the midvein, cellular localization of SoPIN1 is convergent, but along the I1 ring localization SoPIN1 is primarily oriented outward towards the epidermis and shootward toward the incipient cleft between the SAM and the growing primordia (Figure 2: B, E). Opposite the I1 midvein convergence point, SoPIN1 expression remains in the internal layers below the I2 midvein (Figure 2: E).

Consistent with the formation of a radial auxin maxima, expression of DR5 closely follows expression of SoPIN1. DR5 is initially present at the midvein SoPIN1 convergence point of I1 (Figure 1: F), but in later primordia expands around most of the meristem circumference (Figure 1: E, F). After leaf initiation, DR5 expression persists on the top marginal domain of each leaf (Figure 1: F). These data suggest that one aspect of the initiation of a radially encircling leaf is the formation of a radial maxima in the meristem epidermis mediated by SoPIN1.

PIN1b is less canalized during Brachypodium vegetative development

The creation of a radial maxima by SoPIN1 is closely associated with the progressive expansion of PIN1b in the center of the SAM. While PIN1b expression at I2 is biased towards the site of the incipient midvein (Figure 2: D), by I1, expression expands in the internal part of the meristem in a pattern complimentary to SoPIN1 (Figure 2: F). PIN1b is present in the outer layers only at the site of the incipient midvein (Figure 2: F). Remarkably, rather than narrowing into the path of an incipient vascular trace, the continued expansion of PIN1b follows the expansion of the stem, resulting in a conical shape, throughout which cellular localization is primarily rootward (Figure 2: I Arrows). Thus PIN1b during vegetative development lacks many of the obvious characteristics of canalization, while maintaining the connection between subsequent primordia.

The PIN1a pattern in vegetative leaf initiation suggests an uncoupling of vascular and leaf initiation auxin gradients

As discussed in Chapter 2 the early expression of SoPIN1 and PIN1b suggests that these PINs are responsible for the initial auxin gradient required for leaf initiation. During vegetative development I propose that the interaction between radial SoPIN1 convergence and the central un-canalized column of PIN1b act together to mediate the initiation of the encircling organ. As discussed in Chapter 2, both modeling and experimental evidence suggest that PIN canalization may be induced at a threshold auxin concentration (Bayer et al. 2009; Heisler et al. 2005; Scarpella et al. 2006). Thus similar to lemma initiation, I hypothesize that

PIN1a expression may be initially suppressed because PIN1b keeps the auxin concentration below threshold.

The expression pattern of DR5 during vegetative development supports the presence of a low internal auxin concentration in the early stages of leaf initiation. Significant internal DR5 expression is not observed internally until several nodes below the vegetative meristem (Figure 2: J). In the nodes below P3, DR5 expression increases in the internodes and is coincident with a decrease in PIN1b, thus interrupting the continuity of the central PIN1b expression domain around P3/P4 and leading to a complimentary pattern of PIN1b and DR5 across the oldest nodes (Figure 2: J). These data support the idea that high PIN1b expression in the upper nodes keeps the auxin concentration low and that in the lower internodes, as PIN1b expression decreases, the concentration of auxin increases.

In order to follow PIN1a canalization across several nodes, I performed immuno-localization in serial cross sections and mapped this pattern onto data from a staged PIN1b expressing stem (Figure 3: A). Each PIN1a midvein trace begins at the leaf tip and as development proceeds, progressively extends rootward into the stem. Younger I2-P2 PIN1a traces are short and terminate in the central PIN1b expressing domain prior to reaching the next node. In these early leaves, the central column of PIN1b connects the developing midvein of each leaf to the rest of the auxin transport path (Figure 2: I). Thus, consistent with the idea that PIN1a expression is dependent on an auxin concentration threshold, progressive canalization of PIN1a into the stem is coincident with both the increase in DR5 expression and the decrease in PIN1b expression in the lower nodes.

A similar pattern was observed during the development of the secondary leaf veins, called laterals in the grasses. As described above, SoPIN1 expression in the I1 ring persists internally opposite the midvein convergence point just below I2 (Figure 2: E, Right side). By P1, this crescent shape divides into two secondary maxima equidistant from the midvein (Figure 2: G Arrows, Figure 3: B first panel). By P2, SoPIN1 expression resolves further, forming two secondary convergence points on the top of the P2 leaf (“L” in Figure 2: G). PIN1a canalization in each lateral begins at the SoPIN1 convergence points and follows a similar pattern to the midvein. At P1, I observed a very short PIN1a trace that entered the central part of the stem expressing PIN1b and then terminated (Figure 3: A). Remarkably, the points at which SoPIN1 convergence and PIN1a canalization occur during the formation of the first two lateral veins correlates with the further expansion of PIN1b to form a triangular shaped domain in the P1 node (Figure 3: D). At each subsequent node the points of this triangle correspond to the sites of the midvein and first two laterals (Figure 2: H). The triangular shape of PIN1b in the stem persists into the P3 node (Figure 3: D). Thus similar to the midvein, lateral PIN1a traces exiting each leaf are associated with SoPIN1 convergence points and are initially connected to the lower nodes by PIN1b.

Eventual connection of the PIN1a midvein trace to another PIN1a lateral trace occurs late in development, and in this dataset the P3 midvein connects to one of the P4 lateral veins around the P5 node (Figure 3: A, C). It is likely that this connection occurs even earlier, in the P2 leaf, but this was not clearly observed. Similar to the midvein, by P2 the first two PIN1a lateral traces connect with two lateral traces from the P3 leaf (Figure 3: C, double arrows). Once again, the final canalized path of each PIN1a trace is only completed in the lower nodes at the stage where PIN1b expression begins to decrease and DR5 begins to increase.

In summary, canalization of PIN1a, and presumably the final path of the procambium itself, differentiates at a relatively late developmental stage during *Brachypodium* vegetative development. During leaf initiation, the auxin transport path is dominated by SoPIN1 and PIN1b, and prior to P3 the expanding central domain of PIN1b connects subsequent primordia. Below the P3 node, PIN1a traces begin to progressively connect with the existing PIN1a traces of older leaves and this is coincident with an increase in DR5 and a decrease in PIN1b in the internodes. The result is a vein pattern in the stem in which, beginning with the midvein and the first two laterals, the traces of each new primordia nest radially with those of the older leaves (Figure 3: E). These results suggest a temporal uncoupling of auxin transport associated with the differentiation of vascular tissue, and the initial auxin transport gradient that occurs during leaf initiation.

Vegetative leaf vein development

The pattern of vein trace initiation in vegetative leaves largely mirrors the dynamics in the stem. The midvein and first two lateral veins form first (Figure 4: A). Subsequent parallel traces are not associated with changes in the stem PIN1b domain (Figure 3: D) but rather, as discussed in Chapter 2, form de-novo in the expanding gaps between existing canalized veins (Figure 4: C-E). Older vein traces eventually connect at the most distal end of the leaf, but only later in development (Figure 4: E). During the early stages of vein trace formation, DR5 expression persists at the most distal margin, consistent with a broad auxin maxima at the end of each leaf (Figure 4: A, B). Later in development, all three PINs and DR5 overlap in each vein trace (Figure 4: F-I). Thus, in general, vein development is characterized by many individual canalization events proceeding from a large auxin maxima at the most distal leaf margin into the broad PIN1b domain in the stem.

Discussion

PIN subfunctionalization as a plausible mechanism for monocot morphological evolution

Historically, the angiosperms were divided into two groups, the monocots, which have one embryonic leaf, and the dicots, which have two. While modern molecular phylogenies support the monophyletic nature of the monocots, plants with two cotyledons are present in the most basal angiosperms as well as in the more derived eudicots (Bremer et al. 2009). The same is true with other traits, including leaf vein patterning and the arrangement of vascular bundles in the stem. While there are exceptions, in general monocots tend to have parallel, or more precisely, striated vein architecture, while reticulate venation is common in both eudicots and in basal angiosperms (Nelson and Dengler 1997). Similarly, in both basal angiosperms and in the eudicots, the eustele is common. In the eustele the vascular bundles in the stem form a ring, and at the sites where each leaf trace exits the ring there is a gap in the ring circumference (Esau 1977). Unique to the monocots is a stele architecture often described as “scattered” or as an “atactostele” which means “a stele without order”(Figure 3: D) (Zimmermann and Tomlinson 1972). Thus there are several derived traits likely patterned by auxin transport that are unique to the monocots and seem to date from their origin. Furthermore, it is likely that the unique monocot anatomy evolved from a common ancestor with largely eudicot characteristics.

I hypothesize that the functional division of up-the-gradient creation of auxin maxima and with-the-flux creation of auxin sink tissues may provide a basic developmental module on which morphological evolution can occur. Some of the derived aspects of monocot patterning may have been the result of changes in this module. Similar to water moving in a lake or river system auxin transport is to a degree self-organizing, and minor variations in the way auxin moves through the transport system could dramatically alter the positional output, thus altering morphology.

One plausible evolutionary mechanism that could alter auxin gradients is subfunctionalization within the PIN protein family. Subfunctionalization is the process by which recently duplicated genes continue to share the function of the ancestral gene but are, at the same time, relieved of selection and allowed to acquire new functions (Moore and Purugganan 2003; Force et al. 1999). PIN gene duplications may have allowed the evolution of new expression domains and thus new auxin gradients on which developmental processes can be patterned.

Thus it is possible that PIN1a and PIN1b have subfunctionalized the ancestral PIN1 function but over time have acquired new expression domains and responses to auxin concentration. The result is the division of leaf initiation and vascular patterning into an initial PIN1b dependent initiation phase, and a later PIN1a dependent canalization phase. During the first phase, the broad

expression of PIN1b in the central stem suppresses the canalization of PIN1a internally by keeping the internal auxin concentration below the PIN1a threshold. In addition, it is possible that the broad PIN1b expression also suppresses the ability of SoPIN1 to create a defined maximum by shuttling auxin away from the meristem surface evenly across the dome. In this way, PIN1b may act in concert with SoPIN1 to create an encircling maxima and thus an encircling organ. This interaction may be similar to experiments where auxin is added in a broad domain at the top of *Arabidopsis pin1* mutant meristems resulting in the initiation of an encircling organ (Reinhardt et al. 2003). Alternatively it may be similar to *slm1* mutants that also can initiate encircling organs. In this case, the lack of epidermal convergence in the *slm1* mutant may result in ectopic gradients mediated by the remaining PIN1 proteins (Peng and Chen 2011). In either case, I hypothesize that it is the relative contributions of internal sink and epidermal maxima that controls the morphological output. During *Brachypodium* vegetative leaf initiation, the result is the formation of a radial epidermal maxima by SoPIN1 in concert with a large central sink by PIN1b.

During the second phase after leaf initiation, when the auxin concentration increases and PIN1a begins canalization, PIN1b maintains a broad sink at the base of each new leaf. As the stem expands and the overall circumference of each leaf base grows larger, this sink acts to accept more canalized traces from the expanding leaves until later in development when PIN1a canalizes through the lower nodes. In the leaf, DR5 remains high along the most distal edge of the blade, indicating a persistent source of auxin across the entire leaf width. Computer models suggest that this scenario, a broad source and a broad sink, is sufficient to produce parallel veins via canalization (Fujita and Mochizuki 2006). As development proceeds and more leaf veins enter the stem, PIN1b in the center limits maxima formation and canalization to the peripheral tissues by keeping the concentration of auxin in the center of the stem low, and in the later nodes the vasculature of each new leaf ends up nested internally to the vasculature of the previous leaves (Figure 3: D). The result is the formation of the atactostele as well as parallel veins.

In summary, I speculate that during the evolution of the monocots, subfunctionalization of the PIN1 domain by PIN1a and PIN1b caused a heterochronic shift in the timing of leaf vein canalization. The result is that PIN1b and SoPIN1 act during leaf initiation to create a large auxin gradient that only later is canalized by PIN1a to pattern the procambium. My model suggests that different auxin transport events can be uncoupled from the differentiation of the vascular tissues, and similarly that large scale auxin gradients can later become partitioned into smaller domains. Finally, my model may help explain why the atactostele is associated with a tendency toward parallel veins, because inherent to the formation of this type of stele is the formation of a large sink in the central stem.

Materials and Methods

See Materials and Methods for Chapter 2.

Figures

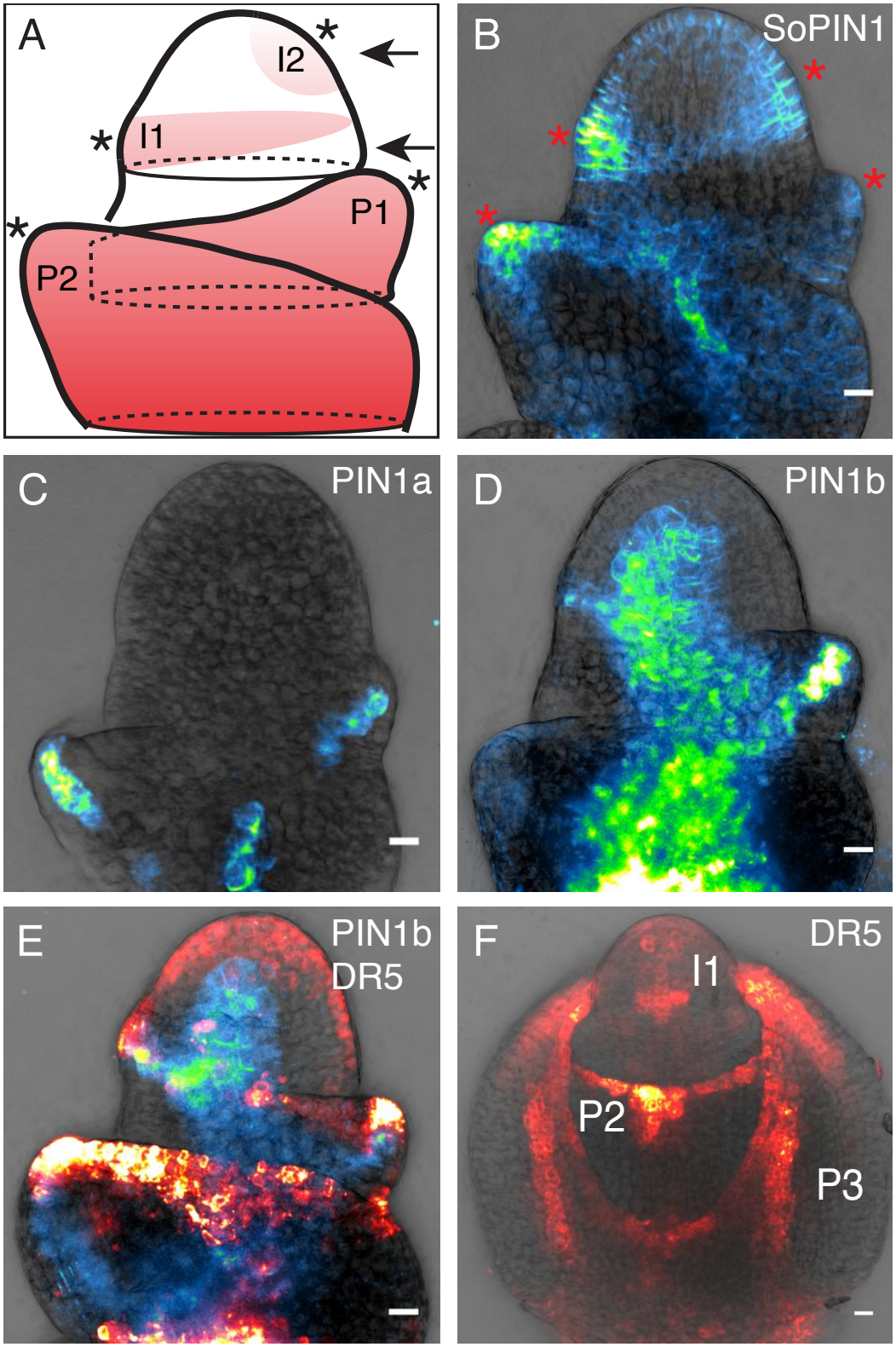

Figure 1

Figure 1: PIN Expression During Vegetative Leaf Initiation. (A) Illustration of longitudinal view of *Brachypodium* vegetative meristem and primordia imaged in B-E. Vegetative leaf primordia I2-P2 are labeled and are colored red. Encircling leaf bases are dotted lines. Arrows mark the level of confocal sections imaged in Figure 2: C-F. (B) SoPIN1. (C) PIN1a. (D) PIN1b. (E) PIN1b and DR5. (F) DR5 only, rotated 90 degrees from A-E and without the P3 leaf removed. Midvein convergence points are marked with asterisks in A-B. Scale Bars: 10μm.

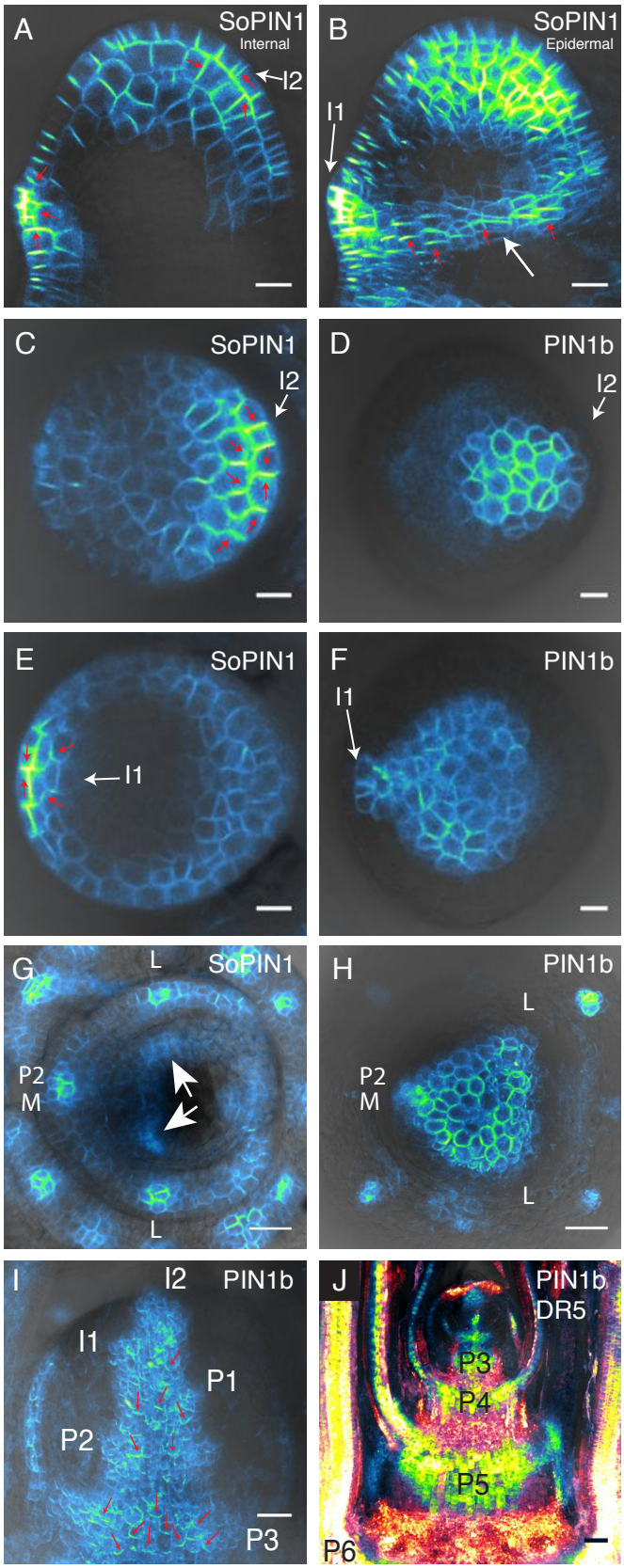
A
SoPIN1
Internal
I2
B
SoPIN1
Epidermal
I1
C
SoPIN1
I2
D
PIN1b
I2
E
SoPIN1
I1
F
PIN1b
I1
G
L
SoPIN1
P2
M
L
H
PIN1b
L
P2
M
L
I
I2
PIN1b
I1
P1
P2
P3
J
PIN1b
DR5
P3
P4
P5
P6

Figure 2

Figure 2: Details of SoPIN1 and PIN1b During Vegetative Leaf Initiation. (A, B, C, E, G) SoPIN1 expression. (A) Internal SoPIN1 confocal section of same dataset as (B). White arrow in B shows I1 ring of SoPIN1 expression. (C-F) show staged confocal cross-sections of SoPIN1 and PIN1b at I2 and I1 primordia. The level of the confocal cross-sections are indicated by arrows in Figure 1: A. (C, D) are more apical sections while (E, F) are lower. (C, E) SoPIN1. (D, F) PIN1b. (G-H) Staged hand sections of SoPIN1 (G) and PIN1b (H) just above the P2 node. The locations of the P2 midvein “P2 M” and first two lateral veins “L” are labeled in (G-H). P1 lateral vein secondary SoPIN1 maxima are indicated by arrows in (G). (I) Hand sectioned stem showing internal PIN1b expression in I2-P3 primordia. (J) A larger hand sectioned stem showing alternating PIN1b and DR5 expression across several nodes, P3-P6 nodes are labeled. Red arrows in (A-C), and (I) show inferred polarity of PIN localization. Scale Bars: 10μm in A-F, 25μm in G-I, and 50μm in J.

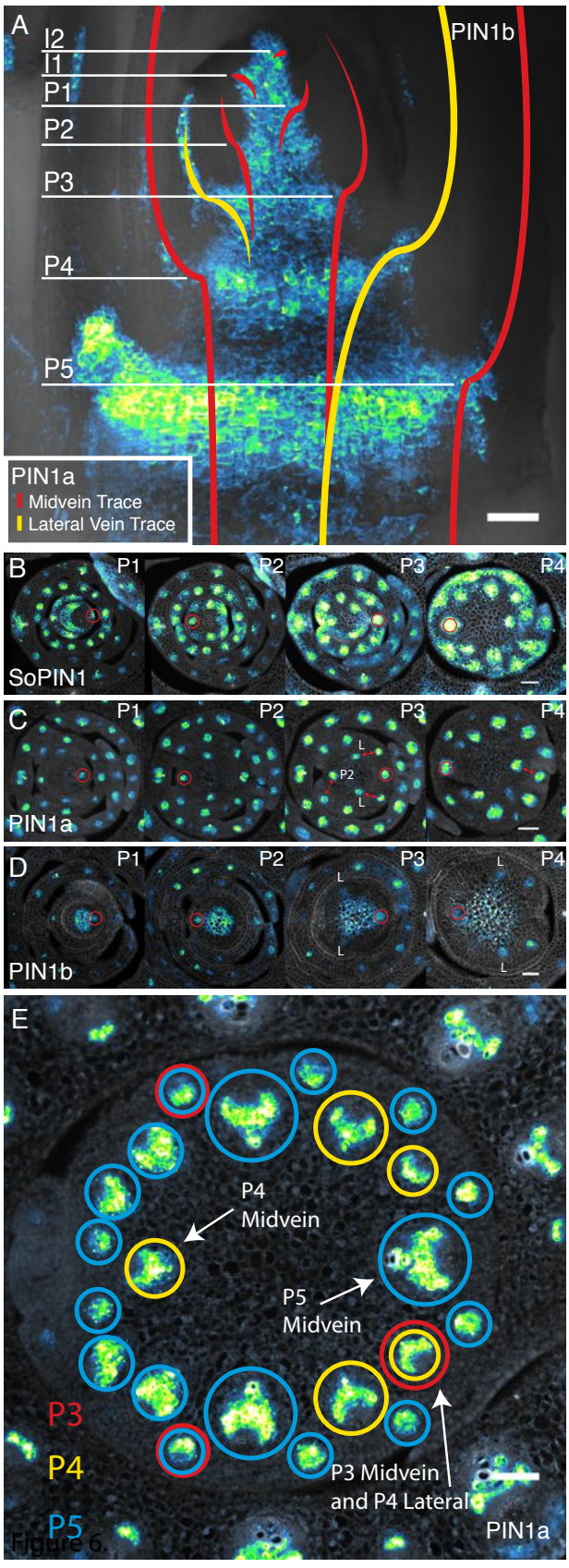

Figure 6.

Figure 3

Figure 3: PIN1b and PIN1a in Vegetative Stem Nodes. (A) PIN1b expression in hand sectioned vegetative stem. PIN1a expression is mapped on top of PIN1a. All PIN1a midvein traces are colored red. The P3 lateral that will connect with the midvein of P2, and the P4 lateral that will connect with the midvein of P3 are colored yellow. Each node I2-P5 is labeled with a horizontal white line indicating the site where the midvein enters the node. (B-D) Anti-GFP immuno-localization of Citrine tagged PINs in vegetative stem cross-sections. In each section the red circle indicates the midvein of consecutive leaves P1-P4, labeled at top right. (B) SoPIN1. (C) PIN1a. Veins that will eventually connect are labeled with double arrows. (D) PIN1b. The points of the central PIN1b triangle that intersect the first 2 lateral traces are labeled with “L”. (E) Anti-GFP immunolocalization of Citrine tagged PIN1a below the vegetative P5 node. Veins derived from P3 are red, from P4 are yellow, and from P5 are blue. Multiple colored circles around a vein indicate that the PIN1a traces connected at a more shootward position. The midveins of P3-P5 are labeled. Scale Bars: 50μm in all.

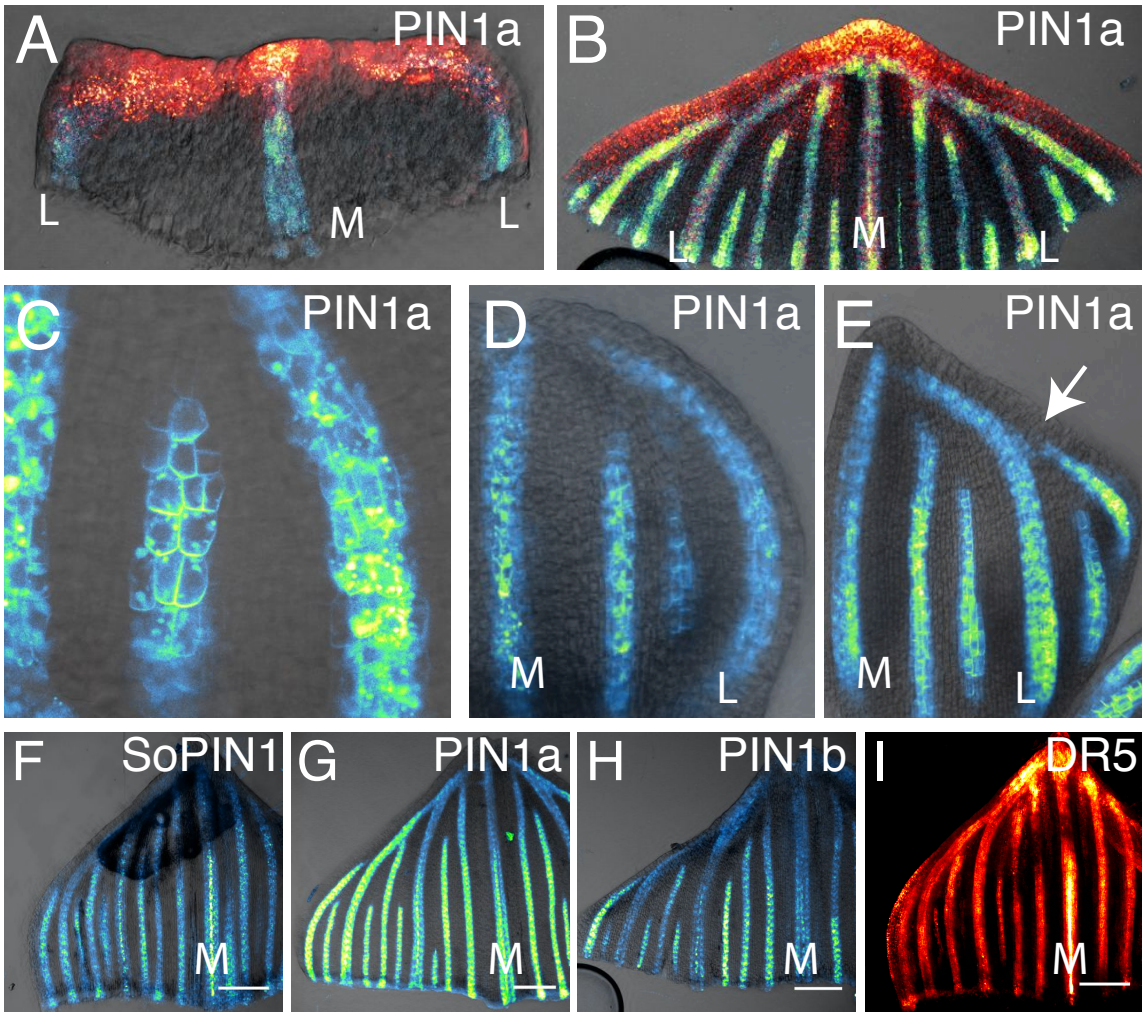

Figure 4

Figure 4: The Timing of Vein Development in *Brachypodium* Vegetative Leaves. (A, B) PIN1a and DR5 expression in a P2 (A) and P5 (B) leaves showing canalized vein traces. (C) PIN1a canalization event between two existing vein traces. (D-E) PIN1a expression in progressively older leaves, shows de-novo vein canalization between existing vein traces. Arrow in (E) shows eventual distal connection of oldest veins. (F-I) Staged P5 half-leaves showing (F) SoPIN1, (G) PIN1a, (H) PIN1b, and (I) DR5 expression. “L” marks the first two lateral veins traces in (A, B, D and E) and “M” marks the midvein trace in (A, B, D, E, F, G, H, I).

Chapter 4: Analysis of PIN amiRNA Knockdown

Introduction

Mutations in members of the *Long-PIN* group disrupt the establishment of auxin gradients and thereby show diverse pleiotropic morphological defects, including organ fusions, an inability to initiate lateral organs, a decrease in leaf morphological complexity, meristem arrest, decreased apical dominance, and even embryo lethality (Barkoulas et al. 2008; Benková et al. 2003; Blilou et al. 2005; Friml et al. 2003; Peng and Chen 2011). Interpreting *Long-PIN* loss-of-function phenotypes is complicated by the finding that mutations in single *Long-PIN* members often lead to compensatory expression changes in other *Long-PIN* members (Vieten et al. 2005; Paponov et al. 2005). Because of this redundancy, multiple PIN mutant combinations are often required to see observable phenotypes. However, genetic interaction of *pin1* with mutants in members of the *PIN3,4,7* clade often have relatively mild phenotypes whereas quadruple *pin1/3/4/7* mutants are embryo or seedling lethal (Friml et al. 2003). This variance in *pin* mutant phenotype can make it difficult to understand the full role of PIN mediated patterning in many tissues.

Another common method used to examine the role of auxin transport in plant development is the use of chemical inhibitors (Mattsson et al. 1999; 2003; Scanlon 2003). Auxin transport inhibitor treatments mimic many of the phenotypes found in PIN mutants, including defects in both leaf initiation and vascular patterning (Reinhardt et al. 2000; 2003). Indeed the auxin transport inhibitor NPA (N-1-naphthylphthalamic acid) directly inhibits PIN1 membrane cycling and in this way disrupts the auxin transport stream (Geldner et al. 2001). Unfortunately the use of NPA has limited utility because it generally inhibits all vesicle trafficking, and thus likely affects many aspects of the cell, not just auxin transport.

While mutants have been characterized in proteins involved in PIN function in the grasses, such as the maize homolog of PINOID (Mcsteen and Hake 2001; Scanlon 2003), no *pin* mutants have been identified in any monocot species. The lack of *pin* mutants may be due to functional redundancy or embryo lethality. In addition, because NPA is difficult to administer to large grass species, it has not been widely used to assess the role of auxin transport in this group. In this Chapter, I first leverage the small size and facile growth conditions of *Brachypodium* to examining phenotypes resulting from NPA treatment. I then describe phenotypes that result from the knockdown of PIN transcripts.

Reverse genetic tools based on small RNAs have proven to be powerful alternatives to traditional forward genetics, especially in cases of genetic redundancy (Waterhouse and Helliwell 2003; Miki and Shimamoto 2004). However, gene knockdown using most double-stranded RNA (dsRNA) technologies is often inconsistent because of the unpredictability of how long hair-pin RNA (hpRNA) constructs will be processed and targeted (Smith et al.

2000; Wesley et al. 2001; Kerschen et al. 2004). While conceptually similar to hpRNA, artificial micro-RNA (amiRNA) mediated gene silencing is far more predictable because only one small piece of the dsRNA hairpin is used for gene targeting allowing greater specificity. In an artificial micro-RNA (amiRNA), genes are targeted by simply replacing the small miRNA targeting sequence of an endogenous miRNA backbone with a sequence corresponding to a gene of interest. Remarkably, the resulting silencing constructs show all of the robust characteristics of traditional miRNA mediated gene regulation (Schwab et al. 2006; Alvarez et al. 2006). Thus, as a preliminary experiment I utilized expression of amiRNAs to knockdown the transcripts of both *PIN1a* and *PIN1b* in *Brachypodium.*

Results

Auxin-transport inhibition disrupts many aspects of *Brachypodium* development

To assess the role of auxin-transport mediated patterning in grass development, I first tested the effect of the auxin transport inhibitor NPA on *Brachypodium*. The phenotypic effect of NPA treatment varied greatly with the concentration used and the method of treatment. Seeds germinated on plates containing a high concentration of NPA often aborted after only initiating a few leaves (Figure 1: B). The leaves that did initiate had severe morphological defects, were short and wide, showed a complete loss of proximal/distal patterning, and had a thickened discolored lamina. No clear distinction between sheath, blade, ligule or auricle tissues was observed in most of the post-embryonic leaves. These leaves were often conical, with a narrowed tip and a wide base. Compared to wild-type (Figure 1: A), branching was also reduced in NPA treated plants at high concentrations (Figure 1: B).

When treated hydroponically at a lower concentration of NPA, plants did not abort, but were still very small (Figure 1: C left). Leaves were shorter and narrower than wild type but had a normal proximal/distal patterning of tissues. While there was a reduced number of spikelets in the inflorescence, these plants tended to branch more at the base, leading to a short bushy phenotype. The overall number of lateral roots and length of the root system was also reduced (Figure 1:C).

Because the range of phenotypes was so dramatic between low and high NPA concentrations, I altered the timing of NPA treatment. When plants were first germinated on normal media then transferred to NPA containing media, I observed a transition of phenotypes from mild to severe in each successive leaf (Figure 1: D). The oldest leaves after treatment were entirely normal, while the next oldest leaves have severely reduced sheath tissue as well as a disrupted lamina at the distal tip (Figure 1: D Inset). Subsequent leaves became shorter, more conical, and lacked distinct auricle and ligule tissue boundaries, similar to

the high NPA concentration treated plants described above (Figure 1: D, Left side). Often the meristem and youngest leaves of axillary branches were completely indistinguishable and these branches terminated with narrow white strands of tissue protruding from a radialized organ surrounding the meristem (Figure 1: D Arrow). In a complimentary experiment, plants were treated with NPA then rescued to normal media. In this experiment, as growth proceeded, leaves became more normal in appearance. Remarkably, for some leaves on rescued plants, all aspects of leaf shape, size, width, and overall tissue patterning were normal, but the ligule/auricle region was reduced or entirely absent, especially near the midrib (Figure 4: F).

Combined, these results suggest a role for auxin transport in many aspects of grass development. Most notably, NPA seemed to inhibit branching and organ initiation at high concentrations, while at low concentrations branch number increased in the lower nodes. These results also show a role for auxin-transport mediated patterning in the proximal/distal axis of the leaf, particularly the formation of the ligule/auricle boundary.

amiRNA-mediated knockdown of *PIN1a and PIN1b* transcripts

As an initial test of the efficacy of amiRNA mediated *PIN* knockdown, and because of possible redundancy, I targeted both *PIN1a* and *PIN1b* transcripts simultaneously using two different amiRNAs. The target sequence of the *Arabidopsis* microRNA *mir319a* (Schwab et al. 2006) was replaced with two different 21nt sequences targeting both PIN transcripts and the resulting amiRNAs were expressed under the constitutive maize *ubiquitin* promoter (Figure 2: A). The two different *PIN* amiRNA constructs will be referred to as *PIN*-amiRNA-A and *PIN*-amiRNA-B for the remainder of this chapter. As a control, and as a second test of the ability of amiRNAs to target multiple related genes in *Brachypodium,* I designed an amiRNA to target the non-essential duplicate *alcohol dehydrogenase* genes *adh1* and *adh2* (Dennis et al. 1985; Freeling et al. 1973; Gaut et al. 1999).

Small-RNA northern blot analysis of the amiRNA transcripts showed that both the *PIN*-amiRNA-A and *adh*-amiRNA hairpins were processed correctly in *Brachypodium* (Figure 2: B). In addition, 5'-RLM RACE cleavage assays showed that both the *PIN*-amiRNA-A and *adh*-amiRNA were capable of guiding target cleavage of both duplicate gene targets at the predicted cleavage sites (Figure 2: C). Finally, qPCR measurement of PIN transcript levels in whole shoots showed a reduction of both *PIN1a* and *PIN1b* transcripts in several *PIN*-amiRNA-A events (Figure 2: D). *PIN*-amiRNA-B plants were not tested for proper amiRNA processing and knockdown.

Unfortunately, while 22 events of the *adh*-amiRNA construct were recovered, only 4 events of the *PIN*-amiRNA-A construct were recovered in my initial round of transformations. In a second attempt to create more transgenic events, the

PIN-amiRNA-A construct was transformed a second time in the Vogel lab. However, again I recovered far fewer events from the *PIN*-amiRNA-A construct than other constructs transformed at the same time, mainly because shoots failed to regenerate from the transformed callus (Jenn Bragg, personal communication). Similarly, only 6 events were recovered of the *PIN*-amiRNA-B construct, and most were phenotypically normal.

Many diverse phenotypes were observed in the recovered *PIN*-amiRNA plants, however, I rarely observed identical phenotypes in several transformation events, and often phenotypes were reduced or entirely absent in the next generation. Because so few events were recovered, it is likely that *PIN* knockdown during regeneration provided strong selection against events that most efficiently reduced *PIN* transcript levels. Indeed there was considerable variation in transcript knockdown between different *PIN*-amiRNA-A events (Figure 2: C). These results suggest that *PIN1a/b* knockdown affects the ability of *Brachypodium* to form regenerated shoots from callus culture and severely limits the utility of *PIN* mediated knockdown using this system. However, as an initial exploration of PIN1/b loss-of-function, in the remainder of this chapter I discuss the phenotypes that were observed in the recovered plants.

PIN1a/b knockdown plants show an increase in branching, meristem arrest, and leaf morphological defects.

Of the four *PIN*-amiRNA-A events recovered from the first round of transformations, 3 showed an increase in shoot branching when compared to the *adh*-amiRNA events. This increase was observed when plants were grown in both short-day and long-day conditions (Figure 3). In the long-day *PIN*-amiRNA-A plants, branch proliferation occurred in the upper nodes after flowering, where axillary buds are normally repressed (Figure 3: B, Inset). In addition, under both short and long-day conditions, flowering was delayed. This was most dramatic in short-day grown plants, which continued to branch with vegetative growth long after control plants had entered senescence (Figure 3: D, Inset).

In the strongest event from this round of transformations, an increase in branching was accompanied by narrow wavy leaves, thin shortened internodes, and aberrant vascular development (Figure 4). The overall number of leaf veins in the blade was reduced, and in some cases there were vascular bundles that appeared absent (Figure 4: E, H, Arrows). Compared to *adh*-amiRNA control plants, the thickness of the leaf was also reduced (Figure 4: A, E). Unfortunately seed set in plants from this strongest event was reduced, and in the next generation the phenotypes were completely lost, possibly due to embryo lethality of *PIN* knockdown.

In the second round of transformations with the *PIN*-amiRNA-A construct, I recovered a single transgenic event that showed severe meristem arrest in the inflorescence (Figure 5: A). Floret number in each spikelet was reduced and

some spikelets aborted after initiating only the sterile bracts (Figure 5: B). Remarkably, immature lemma primordia on arrested spikelet meristems had mature trichomes, whereas wild-type primordia at this stage did not, an indication that they were completely differentiated prior to completing development (Figure 5: D). Thus the meristems in these spikelets appear to have simply stopped the production of new organs and differentiated. Vegetative leaves in this event were sometimes liguleless (Figure 5: F), and many were rumpled and curled with thickened veins (Figure 5: G). One leaf had aberrant margin development and thus formed a complete tube in the sheath (Figure 5: H). Unfortunately no viable seeds were recovered from this event.

Only one of the 6 events recovered from transformation of the *PIN*-amiRNA-B construct showed any discernable phenotype. In this event, vegetative leaves were consistently disrupted. Some leaves were liguleless and lacked clear proximal/distal tissue patterning (Figure 6: A, B). Other leaves had milder phenotypes, but were curled with thickened veins in the blade, similar to leaves from *PIN*-amiRNA-A plants described above (Figure 6: C). In the most severely affected shoots, leaf defects were associated with meristem arrest similar to the strongest *PIN*-amiRNA-A event described above (Figure 6: A Inset). Phenotypes in this event were observed in multiple generations but penetrance and seed set were very low.

SoPIN1 and Dr5 expression but not PIN1b precede ligule/auricle band formation.

Because the ligule/auricle boundary was consistently disrupted in both NPA and *PIN*-amiRNA knockdown plants, I examined the expression of my PIN reporters during ligule/auricle formation. The ligule/auricle boundary begins as a narrow band of small cells known as the pre-ligular band (PLB). After PLB formation, periclinal cell divisions precede outgrowth of the ligule fringe, a flap of tissue at the boundary between the sheath and blade of the leaf (Sylvester et al. 1990; Becraft et al. 1990). In previous work, localization of PIN1a in maize was observed across the leaf prior to PLB formation, suggesting that PIN1a is likely directly involved in patterning these cells (Moon, 2009). I found a similar pattern of SoPIN1 expression during PLB formation in *Brachypodium* leaves. SoPIN1 was expressed across the base of the leaf where the PLB will form and was highest between vein traces (Figure 7: A, B). In contrast, significant PIN1b expression was not detected in the ligule/auricle region prior to PLB formation (Figure 1: C), or after the formation of ligular fringe (Figure 7: D). At the late stages, Dr5 was highly expressed in the ligule fringe, suggesting that SoPIN1 expression in the PLB may act to create a maxima that persists into the ligule itself. Combined, these results suggest that both SoPIN1 and PIN1a may have a role in the formation of the PLB, but that PIN1b likely does not.

Discussion

These results highlight diverse roles for auxin-transport mediated patterning in grass development. The phenotypes I observed in response to both NPA treatment and *PIN1a/b* knockdown varied significantly in severity, from possible embryo or seedling lethality, to increased branching and a loss of the ligule/auricle boundary. Combined with results from *Arabidopsis* where single PIN mutants are mild and multiple mutants are lethal, these results suggest that unexamined roles for auxin transport mediated patterning are yet to be discovered in plant development.

One of the most perplexing findings from this work is that at high NPA concentrations, or in strong *PIN1a/b* knockdown events, branching is severely reduced, whereas at low NPA concentrations and in mild *PIN1a/b* knockdown plants branching is increased compared to wild-type. These phenotypes illustrate the complex interaction between PINs on both a whole plant scale and during organ initiation. In addition to its role in organ initiation, apically derived auxin in the PIN transport stream is known to indirectly inhibit the outgrowth of axillary buds, a phenomena known as apical dominance (Thimann and Skoog 1933; Muller and Leyser 2011). I hypothesize that when PIN function is mildly antagonized there is less apically derived auxin being transported rootward to inhibit bud outgrowth, and the result is a loss of apical dominance and increased branching. This occurs when plants are treated with low NPA concentrations and in most *PIN1a/b* knockdown events, given that plant regeneration was likely to select for events that only partially reduced *PIN1a/b* transcript levels. A similar increase in shoot branching was observed in *PIN1* knockdown plants in rice (Xu et al. 2005). In contrast to these results, a reduced rate of auxin transport mediated by the plant hormone Strigalactone causes reduced branching in *A. thaliana* (Bennett et al. 2006; Crawford et al. 2010), which suggests an opposite relationship between shoot branching and auxin transport. Remarkably, computer modeling of the interaction between auxin transport and bud outgrown reconciles these contradictory findings, and high branching phenotypes can indeed result from either high or low auxin transport in the stem, depending on the timing and location of transport regulation (Prusinkiewicz et al. 2009). This non-linear relationship between auxin transport and apical dominance is a good example of the complex interaction between self-organizing patterning mechanisms and the final phenotypic output.

My results suggests that when PIN function is severely reduced, it affects broader aspects of meristem function, including the maintenance of the spikelet meristem and the ability of plants to regenerate from callus culture. The finding that *PIN1a/b* function is required for shoot regeneration is not surprising, given that up-regulation of *PIN1* in *A. thaliana* is one of the earliest indicators of axis formation during regeneration from callus culture (Gordon et al. 2007) and embryo patterning (Friml et al. 2003). As discussed above in Chapter 2, *pin1* mutants in both *C. hirsuta* and *A. thaliana* show an inability to produce lateral organs in the inflorescence, but in these plants the meristem continues to grow,

resulting in the pin-formed phenotype (Gälweiler et al. 1998; Barkoulas et al. 2008). Remarkably, these pin-formed meristems are still functional, and are capable of organ initiation because apically applied auxin induces organ outgrowth (Reinhardt et al. 2003). Thus only organ initiation, and not basic meristem function is affected in *pin1* mutants in these groups.

In contrast, the meristem appears to simply stop growth entirely and lateral organs differentiate prematurely in severe *PIN1a/b* knockdown plants in *Brachypodium*, indicating that *PIN1a/b* function may be required for the maintenance of the meristem. This phenotype may be the result of an altered ratio of internal canalization, normally mediated by PIN1a/b, and maxima creation by SoPIN1 (Chapter 2). In the absence of PIN1a/b, the internal concentration of auxin may increase, causing SoPIN1 to create spurious maxima that terminate the meristem, almost as if it is an organ itself. In contrast, in the absence of both canalization and maxima creation functions, as is the case in *C. hirsuta* and *A. thaliana,* the meristem may be able to maintain competency because auxin gradients do not form.

Perhaps the most remarkable phenotype observed in my results is the sensitivity of the ligule/auricle boundary to perturbations in auxin-transport. This phenotype was observed in both *PIN*-amiRNA-A and *PIN*-amiRNA-B events as well as in NPA treated plants. Because PIN1b is absent from the PLB, it is likely that the *PIN1a/b* knockdown phenotypes are the result of a loss of PIN1a function. Thus combined with previous observations showing PIN1a at the site of the PLB, these loss-of-function phenotypes strongly support a role for PIN1a in ligule development. In addition, localization of SoPIN1 at the PLB, and Dr5 in the mature ligular fringe, suggests that the formation of an auxin maxima by SoPIN1 may be required for ligule development. As discussed in Chapter 2, PIN mediated patterning is important for proper margin morphogenesis. Perhaps similar genetic programs may regulate margin serrations and ligule formation. Indeed, the missexpression of knotted-like homeobox (KNOX) transcription factors alters both margin development as well as ligule formation (Foster et al. 1999; Chuck et al. 1996; Sinha et al. 1993; L G Smith et al. 1992; Fowler et al. 1996).

Materials and Methods

NPA treatments

NPA was dissolved in DMSO and all control plants were treated with an equal volume of DMSO as mock. Several different treatments were used. In the first treatment, plants were germinated on MS media containing 40µm NPA or DMSO. For hydroponic treatment seeds were germinated on rock wool submerged in 0.5x MS. After germination, plants were suspended on rockwool blocks above 0.5x MS media then treated with 10µm NPA or DMSO. For rescue experiments, seedlings were germinated on paper towels then treated with 5µm

NPA or DMSO in liquid 0.5x MS for 3 weeks. After treatment, plants were rescued to soil for phenotypic analysis.

amiRNA Design

amiRNA backbones were PCR amplified and modified using site-directed mutagenesis using the pRS300 vector containing the *Arabidopsis mir319a* backbone as a template (Schwab et al. 2006). amiRNA target sequences were designed using the WMD design tool: http://wmd3.weigelworld.org/cgi-bin/webapp.cgi. amiRNA backbones were cloned into pENTR-D TOPO. pENTR amiRNA fragments were then recombined into a modified version of the binary vector pH7m24GW that contains a CAT-1 intron. pH7m24GWIntron, accepts two multisite gateway fragments, one promoter fragment, and the pENTR clone containing the amiRNA. For constitutive expression the maize Ubi-1 promoter with the first intron was cloned into the promoter pDONR fragment (Figure 1: A). *Brachypodium* transformation was performed as described (Vogel, Garvin, Leong, and Hayden 2006).

miRNA Northern Blot, miRNA Cleavage Assays and qPCR.

Small RNA analysis was completed as described (Chuck et al. 2007) (Chuck et al. 2008). For qPCR the last node of each branch was collected from 3 week old plants. RNA was extracted using Trizol. Gene specific PIN oligos were designed to span the miRNA cleavage site in order to minimize amplification of cleaved transcripts.

Image Acquisition and Analysis.

Florescent reporter images were captured and processed as described in Chapter 2.

Figures

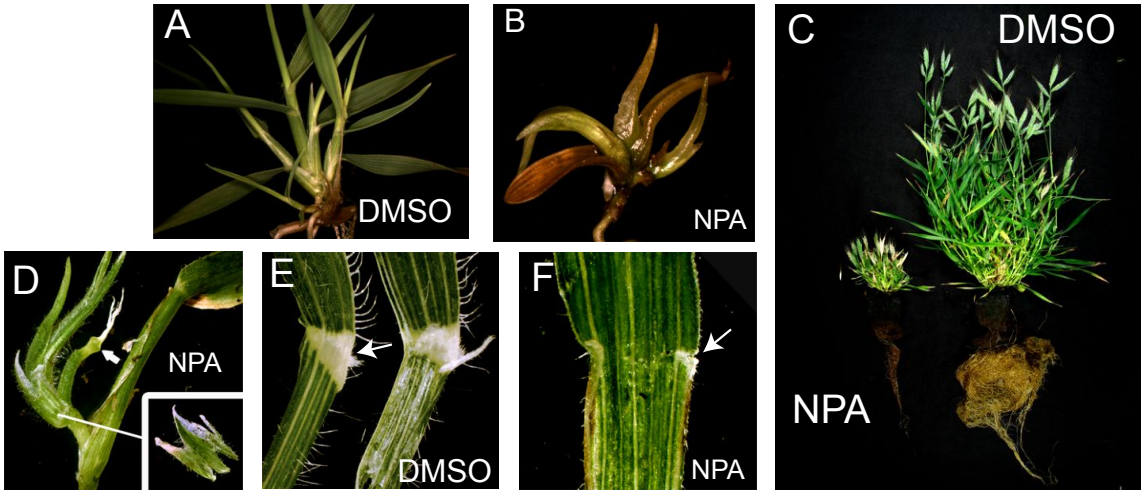

Figure 1

Figure 1: NPA treatment perturbs meristem and leaf patterning. (A, B and C-right) Control plants treated with DMSO. (D, E, F and C-left) treated with NPA. (A) Normal growth of *Brachypodium* 23 days post germination. (B) 40uM NPA treated *Brachypodium* 23 days post germination. (C) Hydroponically grown *Brachypodium*. Right, treated with 10uM NPA. Left, DMSO control. (D) Branch treated with 5uM NPA in liquid culture for 3 weeks then rescued to untreated soil, with inset of first leaf. Arrow pointing to blade/sheath boundary of second leaf. (E) Normal leaf cut in half to show abaxial (left) and adaxial (right) blade/sheath boundary with ligule and auricle (arrow). (F) Liguleless leaf from plant treated with 5uM NPA for 3 weeks then rescued to untreated soil. Arrow shows small domain of auricle tissue near the margin.

A amiRNA T-DNA

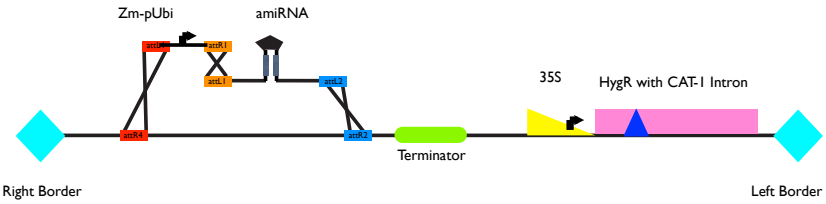

B amiRNA Northern

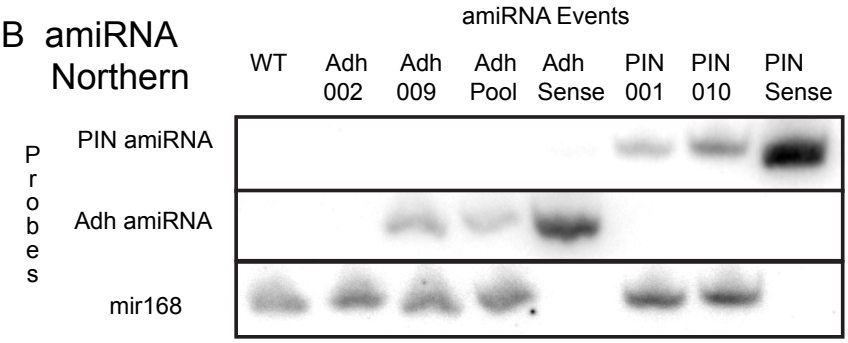

C

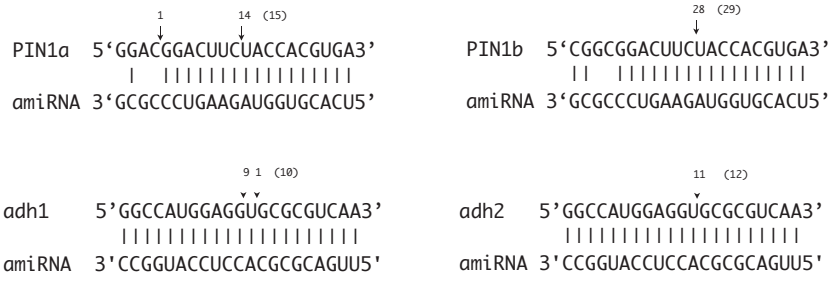

D

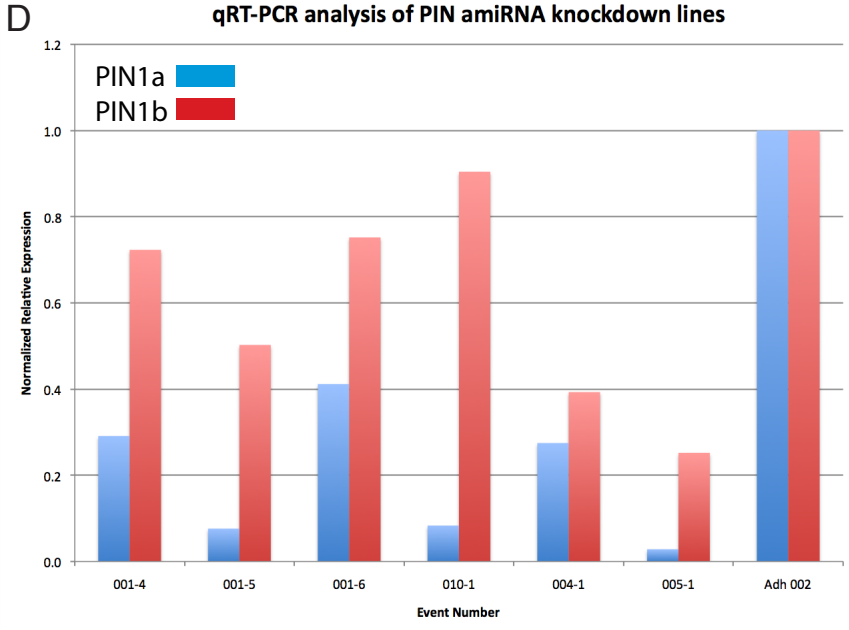

Figure 2

Figure 2: amiRNA-Mediated Knockdown of PIN1a and PIN1b Transcripts. (A) Schematic representation of the amiRNA T-DNA for constitutive amiRNA expression. amiRNAs based on a mutagenized *Arabidopsis mir319a* backbone are recombined into the binary vector using Gateway and placed under the control of the maize *ubiquitin* promoter. (B) Small RNA northern blot of RNA collected from whole shoots showing proper processing of both *adh*-amiRNA and *PIN*-amiRNA-A hairpins. *mir168,* which is constitutively expressed in these tissues is used as a positive loading control. Sense oligos were used as positive probe controls. (C) 5'RLM-RACE cleavage assays showing sites of target cleavage. Arrows show number of cleaved clones at the indicated site out of the total shown in parentheses. (D) qPCR analysis of *PIN*-amiRNA-A mediated knockdown in shoot tissue. All samples are normalized to *PIN* transcripts in an *adh*-amiRNA event. All PIN amiRNA events show a reduction of both *PIN1a* and *PIN1b* transcript levels.

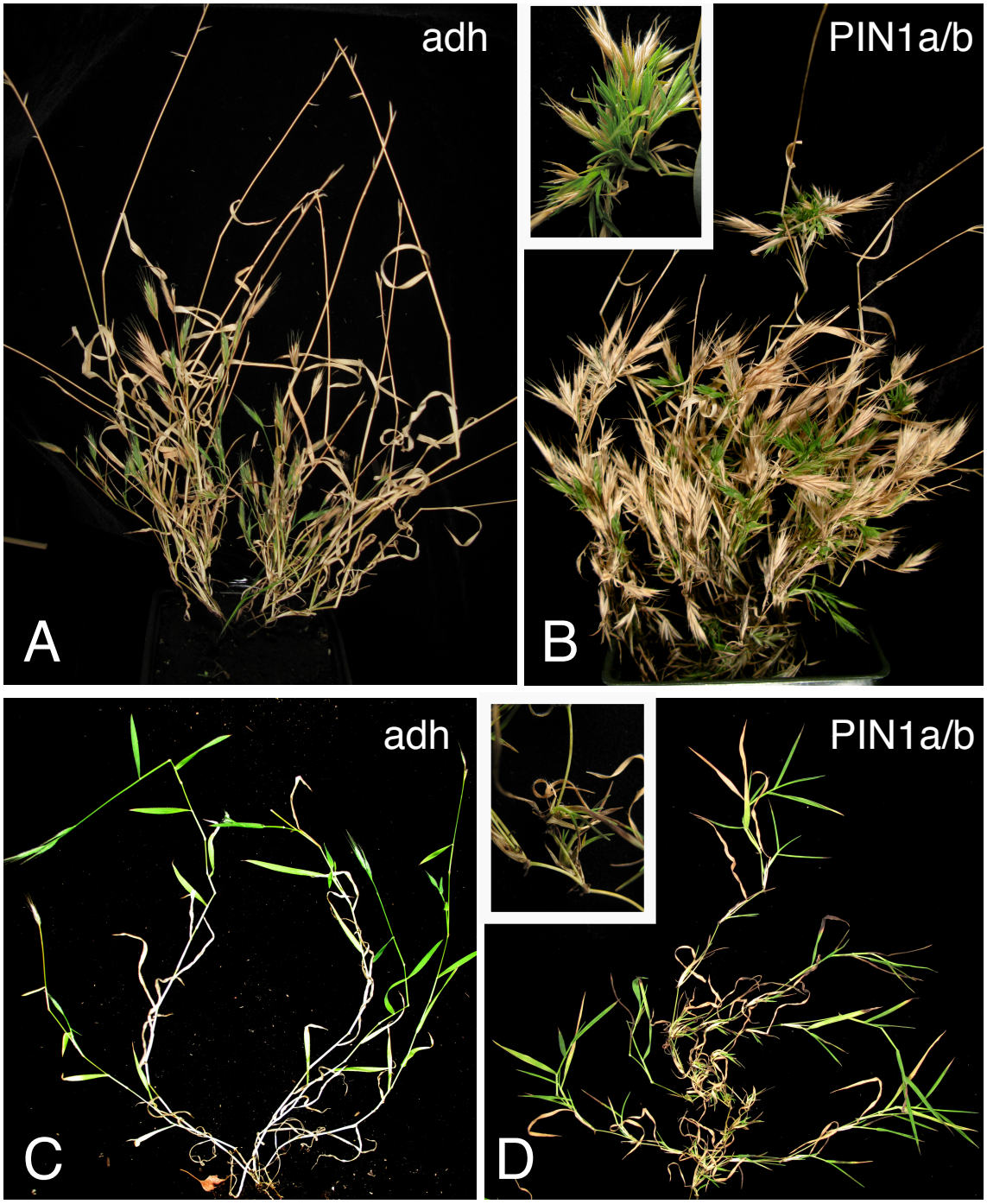

Figure 3

Figure 3: *PIN*-amiRNA-A Knockdown Plants Show Increased Branching. (A-B) Long-day and (C-D) short-day grown *PIN*-amiRNA-A and *adh*-amiRNA plants. (A, C) *adh*-amiRNA control plants. (B, D) *PIN*-amiRNA-A knockdown plants showing an increase in shoot branching. Inset details show branch proliferation at single nodes.

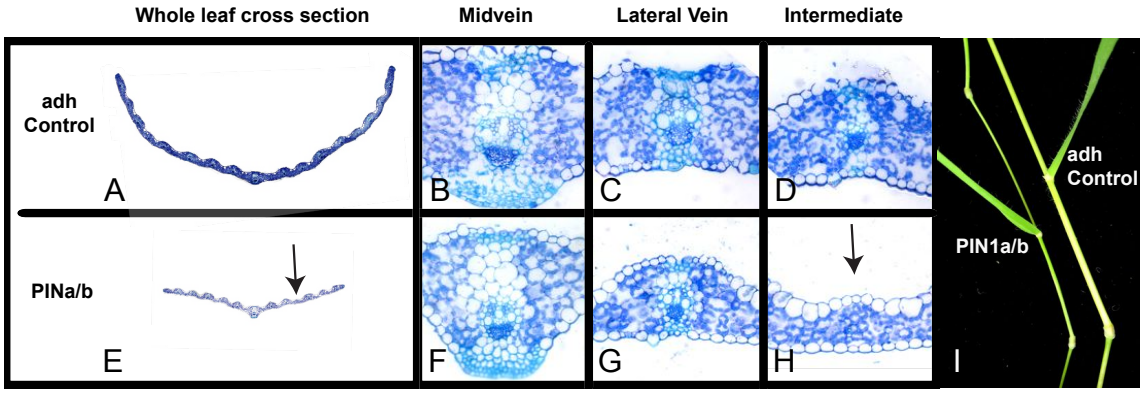

Figure 4

Figure 4: Vascular Defects in *PIN*-amiRNA-A Knockdown Plants. (A-D and I right) *adh*-amiRNA-A control and (E-H and I left) *PIN*-amiRNA-A knockdown leaf and stem defects. (A-D and E-H) Toluidine blue stained plastic sections. (A, E) whole leaf reconstructions. (B-D) and (F-H) Midvein, lateral vein, and Intermediate vein details at 40x. Arrows in (E) and (H) show a vein that is absent in a *PIN*-amiRNA-A leaf. (I) Left shows the thin culm and short nodes of a representative *PIN*-amiRNA-A stem and leaf, right shows representative *adh*-amiRNA control stem and leaf.

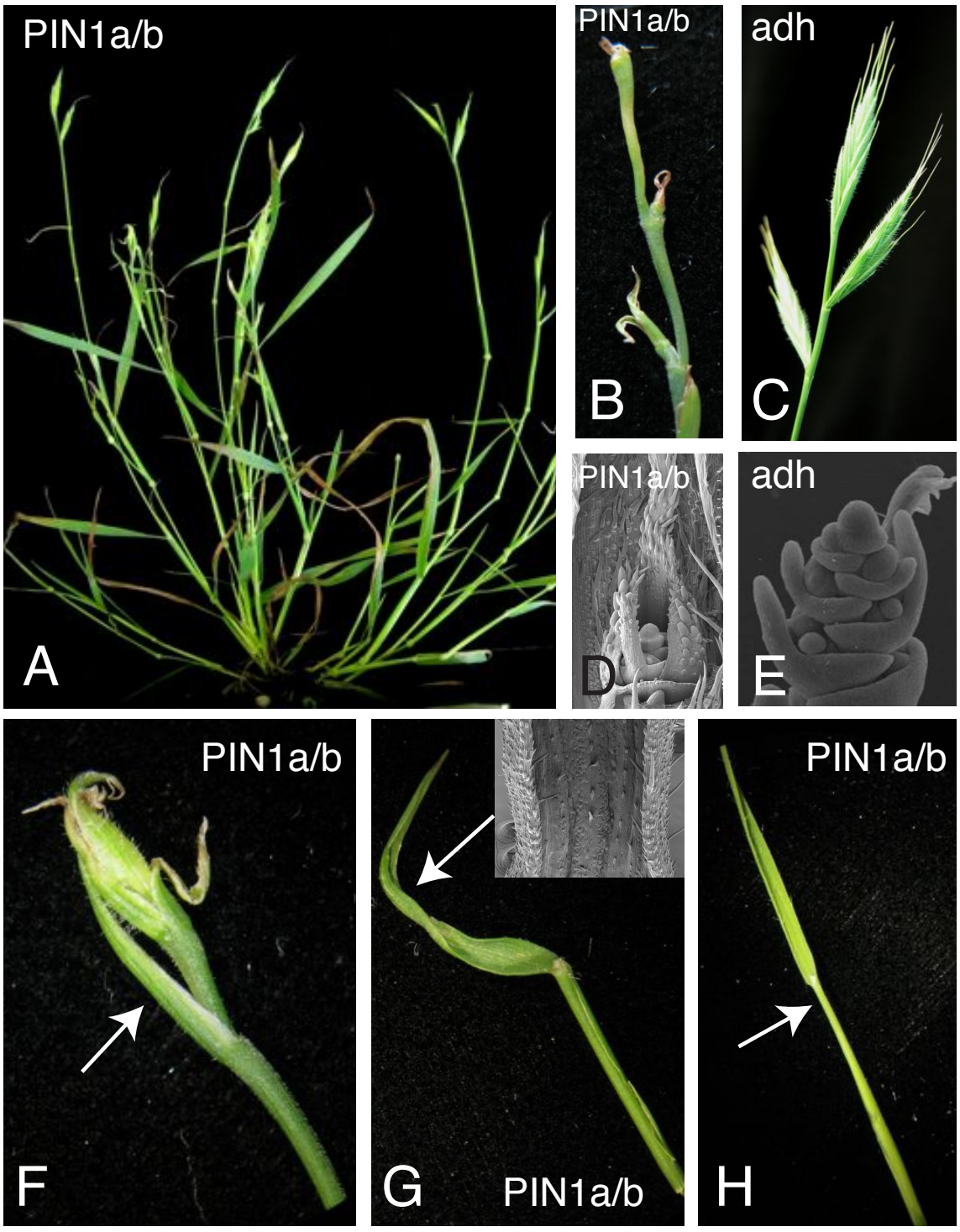

Figure 5

Figure 5: Spikelet Meristem Arrest in *PIN*-amiRNA-A Event. (A) Whole *PIN*-amiRNA-A plant showing reduced spikelet number and barren spikelet nodes. (B) *PIN*-amiRNA-A and showing aborted spikelet meristems compared to *adh*-amiRNA control. (D) SEM detail of aborted *PIN*-amiRNA-A spikelet meristem. (C)

Normal spikelet meristem (courtesy of Clint Whipple). (F) Liguleless leaf in *PIN*-amiRNA-A upper node. (G) Curled leaf with thickened veins in *PIN*-amiRNA-A plant. Inset SEM shows vein thickening. (H) Tube leaf in *PIN*-amiRNA-A plant.

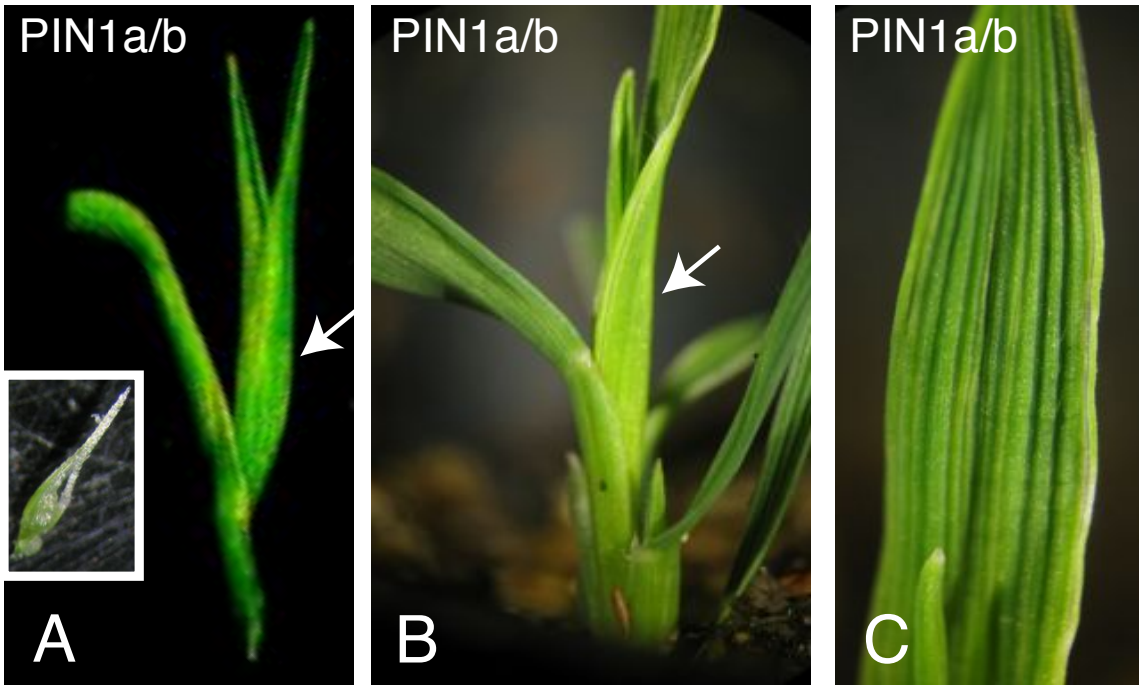

Figure 6

Figure 6: PIN-amiRNA-B Event Shows Liguless Phenotype. (A, B) Liguleless leaves in *PIN*-amiRNA-B shoots. Arrows show liguleless leaves. (A) inset shows arrested meristem in this branch. (C) Thickened leaf veins in *PIN*-amiRNA-B leaf.

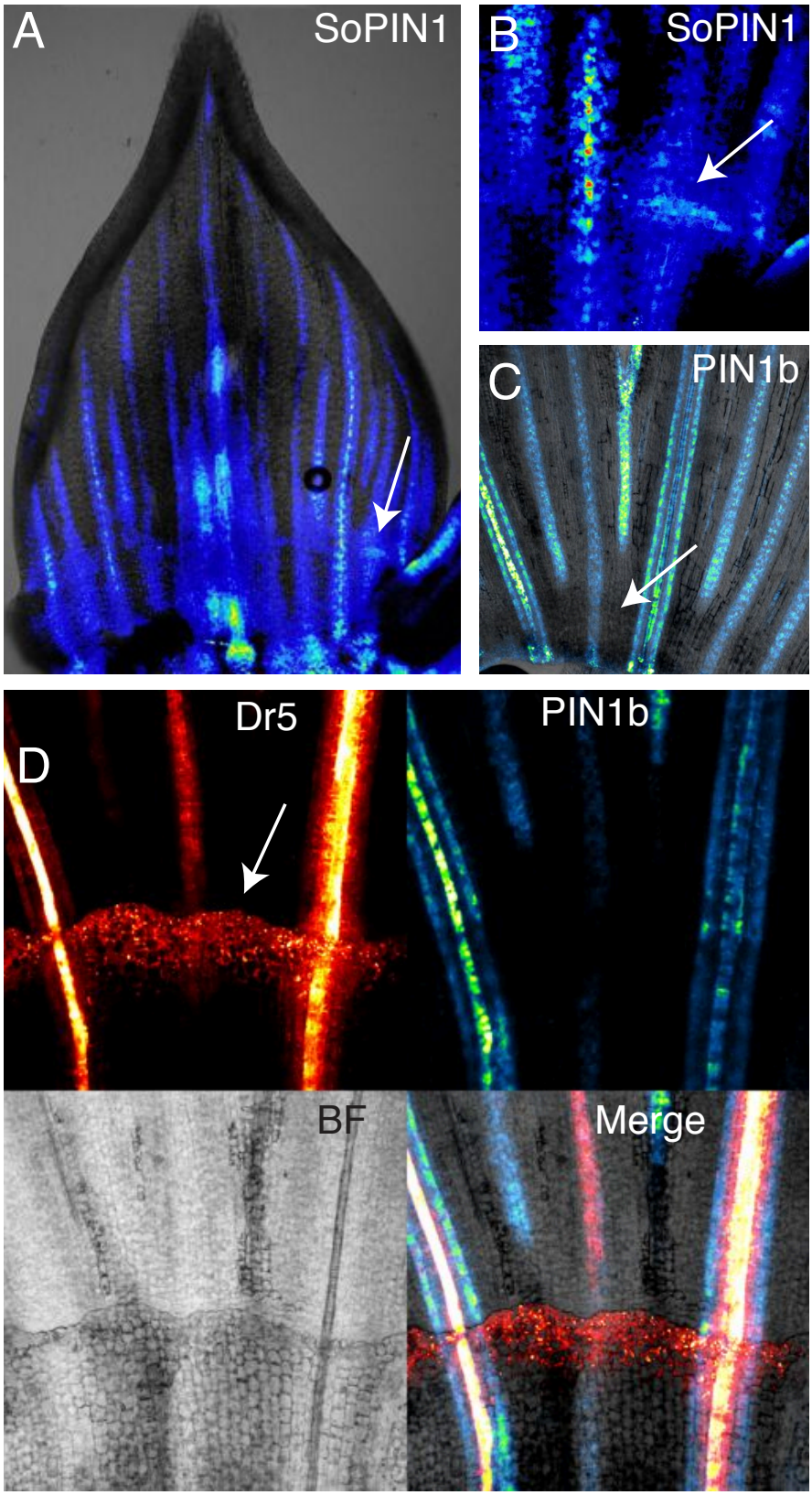

Figure 7

Figure 7: SoPIN1 is expressed in the pre-ligular band but PIN1b is not. (A) SoPIN1 expression at the base of a *Brachypodium* vegetative leaf. Arrow shows expression along the PLB. (B) Detail of SoPIN1 expression along PLB. (C) PIN1b is absent during PLB formation. Arrow shows region of small cells characteristic of PLB formation. (D) Dr5, PIN1b, bright field (BF) and merged images in a developed ligule fringe. Arrow shows high Dr5 expression in the ligule fringe.

Conclusion and Future Research

Combined, this work both advances our understanding of the general principles of auxin-transport mediated patterning, as well as provides specific insight into PIN function in the grasses. Supported by my localization studies in *Brachypodium,* my phylogenetic analysis suggest that the dogma for PIN1 function in *A. thaliana* may not apply to most angiosperms.

The finding that in *Brachypodium,* and possibly in other angiosperms with SoPIN1, up-the-gradient and with-the-flux functions are divided between multiple proteins may help simplify continued research into how PIN is localized in response to auxin. Examination of SoPIN1 alone can help address what mechanisms may control the creation of auxin maxima, while examination of members of the PIN1 clade can help understand canalization. Because I have identified different protein domains in the hydrophilic loops of these proteins, further work can focus on how these domains may regulate the localization of PIN in response to auxin. I hypothesize that heterologous swaps of the variable hydrophilic loop domains between SoPIN1 and PIN1 members will change PIN polarity. If this is the case then a more specific analysis of protein phosphorylation may be able to identify specific residues that are important in regulating up-the-gradient versus with-the-flux PIN localization. Similarly, exchanging the promoter regions of SoPIN1 with PIN1b, for example, may be able to identify whether factors that regulate PIN polarity are dependent on the expression context.

Because *Brachypodium, A. thaliana* and *Medicago* are all efficiently transformed, one way to examine whether PIN1 in *A. thaliana* has acquired up-the-gradient function, and whether the functional division of PIN1 and SoPIN1 in non-*Brassicaceae* eudicots is similar to *Brachypodium,* is to perform heterologous protein swaps between these three groups. For example, if *A. thaliana* PIN1 is able to act up-the-gradient in the SoPIN1 domain as well as with-the-flux in the PIN1a or PIN1b domain, it would support the dual function model for PIN1 in *A. thaliana.* As a complimentary experiment, transformation of PIN1 or SLM1/SoPIN1 from *Medicago* into *A. thaliana* and into *Medicago* itself may show that there is a functional division between these proteins in non-*Brassicaceae* eudicots similar to what I found in *Brachypodium.* Finally, transformation of PIN1b from *Brachypodium* into *Medicago* or *A. thaliana* may alter leaf initiation and vascular patterning and thus provide support for my model that the expansion of the PIN1b domain in monocots is related to novel monocot morphologies.

The antibodies raised to maize PIN1a, PIN1b, and SoPIN1 will likely cross-react with members of the PIN1 and SoPIN1 clades in other species. Thus immunolocalization using these antibodies on species across the angiosperms may help provide a more generalized view of PIN function. Simply showing that up-the-gradient and with-the-flux functions are mediated by separate PIN proteins in diverse species across the angiosperms will provide considerable

support for my model. Similarly, I hypothesize that the expanded domain of PIN1b may be a monocot specific trait, and these antibodies can be used to determine if the division of PIN1a and PIN1b exists in other monocot species.

Of obvious importance to understanding the functions of PIN1a, PIN1b and SoPIN1 in the grasses is the identification of loss-of-function mutants. In maize I have so far identified *Mutator* transposon insertions in *PIN1a* and *PIN1b*, while our collaborators at Pioneer Hybrid have identified insertions in *SoPIN1* and *PIN1c*. Work on these mutants is ongoing, and should provide valuable phenotypic data on the function of these PINs in grass development.

My work so far has shown that the *Brachypodium* spikelet meristem is particularly well suited for live florescent imaging. Further work will focus on creating new reporter lines to detect the activity of other plant hormones as well as mark specific cell domains. I have already created a version of a new reporter for auxin concentration that should compliment my previous work on PIN proteins and Dr5. Using these tools, further analysis of PIN localization and auxin activity during the formation of the PLB will be valuable to understanding the role of auxin transport in auricle and ligule development. In addition, my preliminary analysis suggests that PIN1a, PIN1b and SoPIN1 have unique expression domains during both embryo and root development, but further imaging is needed.

In conclusion I believe that this work justifies further examination of the PIN family across the angiosperms and may help provide a general model for the evolution of morphological diversity in plants.

References

Abas L, Benjamins R, Malenica N, Paciorek T, Wirniewska J, Moulinier-Anzola J, Sieberer T, Friml J, and Luschnig C. 2006. Intracellular trafficking and proteolysis of the Arabidopsis auxin-efflux facilitator PIN2 are involved in root gravitropism. *Nat Cell Biol* **8**: 249–256.

Alvarez JP, Pekker I, Goldshmidt A, Blum E, Amsellem Z, and Eshed Y. 2006. Endogenous and synthetic microRNAs stimulate simultaneous, efficient, and localized regulation of multiple targets in diverse species. *Plant Cell* **18**: 1134–1151.

Barkoulas M, Hay A, Kougioumoutzi E, and Tsiantis M. 2008. A developmental framework for dissected leaf formation in the Arabidopsis relative Cardamine hirsuta. *Nat Genet* **40**: 1136–1141.

Bayer EM, Smith RS, Mandel T, Nakayama N, Sauer M, Prusinkiewicz P, and Kuhlemeier C. 2009. Integration of transport-based models for phyllotaxis and midvein formation. *Genes Dev* **23**: 373–384.

Becraft PW, Bongard-Pierce DK, Sylvester AW, Poethig RS, and Freeling M. 1990. The liguleless-1 gene acts tissue specifically in maize leaf development. *Dev Biol* **141**: 220–232.

Benková E, Michniewicz M, Sauer M, Teichmann T, Seifertová D, Jürgens G, and Friml J. 2003. Local, efflux-dependent auxin gradients as a common module for plant organ formation. *Cell* **115**: 591–602.

Bennett T, Sieberer T, Willett B, Booker J, Luschnig C, and Leyser O. 2006. The Arabidopsis MAX pathway controls shoot branching by regulating auxin transport. *Curr Biol* **16**: 553–563.

Bilsborough GD, Runions A, Barkoulas M, Jenkins HW, Hasson A, Galinha C, Laufs P, Hay A, Prusinkiewicz P, and Tsiantis M. 2011. Model for the regulation of Arabidopsis thaliana leaf margin development. *Proc Natl Acad Sci USA* **108**: 3424–3429.

Blilou I, Xu J, Wildwater M, Willemsen V, Paponov I, Friml J, Heidstra R, Aida M, Palme K, and Scheres B. 2005. The PIN auxin efflux facilitator network controls growth and patterning in Arabidopsis roots. *Nature* **433**: 39–44.

Bremer B, Bremer K, Chase MW, Fay MF, Reveal JL, Soltis DE, Soltis PS, Stevens PF, Anderberg AA, Moore MJ, et al. 2009. An update of the Angiosperm Phylogeny Group classification for the orders and families of flowering plants: APG III. *Bot J Linn Soc* **161**: 105–121.

Brooks L, Strable J, Zhang X, Ohtsu K, Zhou R, Sarkar A, Hargreaves S, Elshire

RJ, Eudy D, Pawlowska T, et al. 2009. Microdissection of shoot meristem functional domains. *PLoS Genet* **5**: e1000476.

Carraro N, Forestan C, Canova S, Traas J, and Varotto S. 2006. ZmPIN1a and ZmPIN1b encode two novel putative candidates for polar auxin transport and plant architecture determination of maize. *Plant Physiol* **142**: 254–264.

Chen R, Hilson P, Sedbrook JC, Rosen E, Caspar T, and Masson PH. 1998. The arabidopsis thaliana AGRAVITROPIC 1 gene encodes a component of the polar-auxin-transport efflux carrier. *Proc Natl Acad Sci USA* **95**: 15112–15117.

Chuck G, Lincoln C, and Hake S. 1996. KNAT1 induces lobed leaves with ectopic meristems when overexpressed in Arabidopsis. *Plant Cell* **8**: 1277–1289.

Chuck G, Meeley R, and Hake S. 2008. Floral meristem initiation and meristem cell fate are regulated by the maize AP2 genes ids1 and sid1. *Development* **135**: 3013–3019.

Chuck G, Meeley R, Irish E, Sakai H, and Hake S. 2007. The maize tasselseed4 microRNA controls sex determination and meristem cell fate by targeting Tasselseed6/indeterminate spikelet1. *Nat Genet* **39**: 1517–1521.

Crawford S, Shinohara N, Sieberer T, Williamson L, George G, Hepworth J, Muller D, Domagalska MA, and Leyser O. 2010. Strigolactones enhance competition between shoot branches by dampening auxin transport. *Development* **137**: 2905–2913.

Dhonukshe P, Huang F, Galván-Ampudia CS, Mähönen AP, Kleine-Vehn J, Xu J, Quint A, Prasad K, Friml J, Scheres B, et al. 2010. Plasma membrane-bound AGC3 kinases phosphorylate PIN auxin carriers at TPRXS(N/S) motifs to direct apical PIN recycling. *Development* **137**: 3245–3255.

Draper J, Mur LA, Jenkins G, Ghosh-Biswas GC, Bablak P, Hasterok R, and Routledge AP. 2001. Brachypodium distachyon. A New Model System for Functional Genomics in Grasses. *Plant Physiol* **127**: 1539–1555.

Esau K. 1977. *Anatomy of Seed Plants, 2nd edition*. 2nd ed. John Wiley & Sons Inc.

Force A, Lynch M, Pickett FB, Amores A, Yan YL, and Postlethwait J. 1999. Preservation of duplicate genes by complementary, degenerative mutations. *Genetics* **151**: 1531–1545.

Foster T, Yamaguchi J, Wong BC, Veit B, and Hake S. 1999. Gnarley1 is a dominant mutation in the knox4 homeobox gene affecting cell shape and identity. *Plant Cell* **11**: 1239–1252.

Fowler JE, Muehlbauer GJ, and Freeling M. 1996. Mosaic analysis of the liguleless3 mutant phenotype in maize by coordinate suppression of mutator-insertion alleles. *Genetics* **143**: 489–503.

Freeling M. 2009. Bias in plant gene content following different sorts of duplication: tandem, whole-genome, segmental, or by transposition. *Annual Review of Plant Biology* **60**: 433–453.

Freeling M, and Subramaniam S. 2009. Conserved noncoding sequences (CNSs) in higher plants. *Curr Opin Plant Biol* **12**: 126–132.

Friml J, Benková E, Blilou I, Wisniewska J, Hamann T, Ljung K, Woody S, Sandberg G, Scheres B, Jürgens G, and Palme K. 2002. AtPIN4 mediates sink-driven auxin gradients and root patterning in Arabidopsis. *Cell* **108**: 661–673.

Friml J, Vieten A, Sauer M, Weijers D, Schwarz H, Hamann T, Offringa R, and Jürgens G. 2003. Efflux-dependent auxin gradients establish the apical-basal axis of Arabidopsis. *Nature* **426**: 147–153.

Friml J, Wisniewska J, Benková E, Mendgen K, and Palme K. 2002. Lateral relocation of auxin efflux regulator PIN3 mediates tropism in Arabidopsis. *Nature* **415**: 806–809.

Fujita H, and Mochizuki A. 2006. The origin of the diversity of leaf venation pattern. *Dev Dyn* **235**: 2710–2721.

Gallavotti A, Yang Y, Schmidt R, and Jackson D. 2008. The relationship between auxin transport and maize branching. *Plant Physiol*.

Garnett P, Steinacher A, Stepney S, Clayton R, and Leyser O. 2010. Computer simulation: the imaginary friend of auxin transport biology. *Bioessays* **32**: 828–835.

Gaut BS, Peek AS, Morton BR, and Clegg MT. 1999. Patterns of genetic diversification within the Adh gene family in the grasses (Poaceae). *Mol Biol Evol* **16**: 1086–1097.

Gälweiler L, Guan C, Müller A, Wisman E, Mendgen K, Yephremov A, and Palme K. 1998. Regulation of polar auxin transport by AtPIN1 in Arabidopsis vascular tissue. *Science* **282**: 2226–2230.

Geldner N, Friml J, Stierhof YD, Jürgens G, and Palme K. 2001. Auxin transport inhibitors block PIN1 cycling and vesicle trafficking. *Nature* **413**: 425–428.

Gordon SP, Heisler MG, Reddy GV, Ohno C, Das P, and Meyerowitz EM. 2007. Pattern formation during de novo assembly of the Arabidopsis shoot meristem. *Development* **134**: 3539–3548.

Gray A. 1879. *Structural Botany*. Macmillan and Co., New York.

Hay A, and Tsiantis M. 2006. The genetic basis for differences in leaf form between Arabidopsis thaliana and its wild relative Cardamine hirsuta. *Nat Genet* **38**: 942–947.

Hay A, Barkoulas M, and Tsiantis M. 2006. ASYMMETRIC LEAVES1 and auxin activities converge to repress BREVIPEDICELLUS expression and promote leaf development in Arabidopsis. *Development* **133**: 3955–3961.

Heisler MG, Ohno C, Das P, Sieber P, Reddy GV, Long JA, and Meyerowitz EM. 2005. Patterns of auxin transport and gene expression during primordium development revealed by live imaging of the Arabidopsis inflorescence meristem. *Curr Biol* **15**: 1899–1911.

Huang F, Zago MK, Abas L, van Marion A, Galván-Ampudia CS, and Offringa R. 2010. Phosphorylation of conserved PIN motifs directs Arabidopsis PIN1 polarity and auxin transport. *Plant Cell* **22**: 1129–1142.

Inada DC. 2003. Conserved Noncoding Sequences in the Grasses. *Genome Res* **13**: 2030–2041.

Jönsson H, Heisler MG, Shapiro BE, Meyerowitz EM, and Mjolsness E. 2006. An auxin-driven polarized transport model for phyllotaxis. *Proc Natl Acad Sci USA* **103**: 1633–1638.

Kaplinsky NJ, Braun DM, Penterman J, Goff SA, and Freeling M. 2002. Utility and distribution of conserved noncoding sequences in the grasses. *Proc Natl Acad Sci USA* **99**: 6147–6151.

Kellogg EA. 2001. Evolutionary history of the grasses. *Plant Physiol* **125**: 1198–1205.

Kerschen A, Napoli CA, Jorgensen RA, and Müller AE. 2004. Effectiveness of RNA interference in transgenic plants. *FEBS Lett.* **566**: 223–228.

Koenig D, Bayer E, Kang J, Kuhlemeier C, and Sinha N. 2009. Auxin patterns Solanum lycopersicum leaf morphogenesis. *Development* **136**: 2997–3006.

Kramer E. 2004. PIN and AUX/LAX proteins: their role in auxin accumulation. *Trends Plant Sci* **9**: 578–582.

Krecek P, Skůpa P, Libus J, Naramoto S, Tejos R, Friml J, and Zazímalová E. 2009. The PIN-FORMED (PIN) protein family of auxin transporters. *Genome Biol* **10**: 249.

Luschnig C, Gaxiola RA, Grisafi P, and Fink GR. 1998. EIR1, a root-specific protein involved in auxin transport, is required for gravitropism in Arabidopsis

thaliana. *Genes Dev* **12**: 2175–2187.

Lyons E, and Freeling M. 2008. How to usefully compare homologous plant genes and chromosomes as DNA sequences. *Plant J* **53**: 661–673.

Mattsson J, Ckurshumova W, and Berleth T. 2003. Auxin signaling in Arabidopsis leaf vascular development. *Plant Physiol* **131**: 1327–1339.

Mattsson J, Sung ZR, and Berleth T. 1999. Responses of plant vascular systems to auxin transport inhibition. *Development* **126**: 2979–2991.

Mcsteen P, and Hake S. 2001. barren inflorescence2 regulates axillary meristem development in the maize inflorescence. *Development* **128**: 2881–2891.

Miki D, and Shimamoto K. 2004. Simple RNAi vectors for stable and transient suppression of gene function in rice. *Plant Cell Physiol* **45**: 490–495.

MITCHISON G. 1980. Model for Vein Formation in Higher-Plants. *P Roy Soc Lond B Bio* **207**: 79–109.

MITCHISON G. 1981. The Polar Transport of Auxin and Vein Patterns in Plants. *Philos T Roy Soc B* **295**: 461–&.

Moore RC, and Purugganan MD. 2003. The early stages of duplicate gene evolution. *Proc Natl Acad Sci USA* **100**: 15682–15687.

Mravec J, Skůpa P, Bailly A, Hoyerová K, Krecek P, Bielach A, Petrásek J, Zhang J, Gaykova V, Stierhof Y-D, et al. 2009. Subcellular homeostasis of phytohormone auxin is mediated by the ER-localized PIN5 transporter. *Nature* **459**: 1136–1140.

Muller D, and Leyser O. 2011. Auxin, cytokinin and the control of shoot branching. *Ann Bot-London* **107**: 1203–1212.

Müller A, Guan C, Gälweiler L, Tänzler P, Huijser P, Marchant A, Parry G, Bennett M, Wisman E, and Palme K. 1998. AtPIN2 defines a locus of Arabidopsis for root gravitropism control. *EMBO J* **17**: 6903–6911.

Nelson T, and Dengler N. 1997. Leaf vascular pattern formation. *Plant Cell*.

Okada K, Ueda J, Komaki M, Bell C, and Shimura Y. 1991. Requirement of the Auxin Polar Transport System in Early Stages of Arabidopsis Floral Bud Formation. *Plant Cell* **3**: 677–684.

Paponov IA, Teale WD, Trebar M, Blilou I, and Palme K. 2005. The PIN auxin efflux facilitators: evolutionary and functional perspectives. *Trends Plant Sci* **10**: 170–177.

Peng J, and Chen R. 2011. Auxin efflux transporter MtPIN10 regulates compound leaf and flower development in Medicago truncatula. *Plant Signal Behav* **6**.

Petrásek J, and Friml J. 2009. Auxin transport routes in plant development. *Development* **136**: 2675–2688.

Petrásek J, Mravec J, Bouchard R, Blakeslee JJ, Abas M, Seifertová D, Wisniewska J, Tadele Z, Kubes M, Covanová M, et al. 2006. PIN proteins perform a rate-limiting function in cellular auxin efflux. *Science* **312**: 914–918.

Prusinkiewicz P, Crawford S, Smith RS, Ljung K, Bennett T, Ongaro V, and Leyser O. 2009. Control of bud activation by an auxin transport switch. *Proc Natl Acad Sci USA* **106**: 17431–17436.

Raven J. 1975. Transport of indoleacetic-acid in plant-cells in relation to ph and electrical potential gradients, and its significance for polar iaa transport. *New Phytol* **74**: 163–172.

Reinhardt D, Mandel T, and Kuhlemeier C. 2000. Auxin regulates the initiation and radial position of plant lateral organs. *Plant Cell* **12**: 507–518.

Reinhardt D, Pesce E-R, Stieger P, Mandel T, Baltensperger K, Bennett M, Traas J, Friml J, and Kuhlemeier C. 2003. Regulation of phyllotaxis by polar auxin transport. *Nat Cell Biol* **426**: 255–260.

Rubery PH, and Sheldrake AR. 1974. Carrier-mediated auxin transport. *Planta* **118**: 101.

Rubery PH, and Sheldrake AR. 1973. Effect of pH and surface charge on cell uptake of auxin. *Nature New Biol* **244**: 285–288.

Sachs T. 1991. Cell polarity and tissue patterning in plants. *Development* 83–93.

Sachs T. 1969. Polarity and induction of organized vascular tissues. *Ann Bot-London* **33**: 263–&.

Sachs T. 1981. The Control of the Patterned Differentiation of Vascular Tissues. *Adv Bot Res* **9**: 151–262.

Scanlon MJ. 2003. The polar auxin transport inhibitor N-1-naphthylphthalamic acid disrupts leaf initiation, KNOX protein regulation, and formation of leaf margins in maize. *Plant Physiol* **133**: 597–605.

Scarpella E, Marcos D, Friml J, and Berleth T. 2006. Control of leaf vascular patterning by polar auxin transport. *Genes Dev* **20**: 1015–1027.

Schwab R, Ossowski S, Riester M, Warthmann N, and Weigel D. 2006. Highly

specific gene silencing by artificial microRNAs in Arabidopsis. *Plant Cell* **18**: 1121–1133.

Shantz H. 1954. The place of grasslands in the Earth's cover. *Ecology*.

Sharman B. 1942. Developmental anatomy of the shoot of Zea mays L. *Ann Bot-London* **6**: 245–282.

Sinha NR, Williams RE, and Hake S. 1993. Overexpression of the maize homeo box gene, KNOTTED-1, causes a switch from determinate to indeterminate cell fates. *Genes Dev* **7**: 787–795.

Smith LG, Greene B, Veit B, and Hake S. 1992. A dominant mutation in the maize homeobox gene, Knotted-1, causes its ectopic expression in leaf cells with altered fates. *Development* **116**: 21–30.

Smith NA, Singh SP, Wang MB, Stoutjesdijk PA, Green AG, and Waterhouse PM. 2000. Total silencing by intron-spliced hairpin RNAs. *Nature* **407**: 319–320.

Smith RS. 2006. A plausible model of phyllotaxis. *Proc Natl Acad Sci USA* **103**: 1301–1306.

Somerville C. 2006. The Billion-Ton Biofuels Vision. *Science* **312**: 1277–1277.

Sylvester AW, Cande WZ, and Freeling M. 1990. Division and differentiation during normal and liguleless-1 maize leaf development. *Development* **110**: 985–1000.

Tang J, Donnelly P, and Dengler N. 2003. Primary vascular pattern and expression of ATHB-8 in shoots of Arabidopsis. *New Phytologist*.

Thimann KV, and Skoog F. 1933. Studies on the Growth Hormone of Plants: III. The Inhibiting Action of the Growth Substance on Bud Development. *Proc Natl Acad Sci USA* **19**: 714–716.

Vain P, Worland B, Thole V, McKenzie N, Alves SC, Opanowicz M, Fish LJ, Bevan MW, and Snape JW. 2008. Agrobacterium-mediated transformation of the temperate grass Brachypodium distachyon (genotype Bd21) for T-DNA insertional mutagenesis. *Plant Biotechnol J* **6**: 236–245.

Vieten A, Vanneste S, Wisniewska J, Benková E, Benjamins R, Beeckman T, Luschnig C, and Friml J. 2005. Functional redundancy of PIN proteins is accompanied by auxin-dependent cross-regulation of PIN expression. *Development* **132**: 4521–4531.

Vogel J, and Hill T. 2008. High-efficiency Agrobacterium-mediated transformation of Brachypodium distachyon inbred line Bd21-3. *Plant Cell Rep* **27**: 471–478.

Vogel JP, Garvin DF, Leong OM, and Hayden DM. 2006. Agrobacterium-mediated transformation and inbred line development in the model grass Brachypodium distachyon. *Plant Cell Tiss Organ Cult* **84**: 100179–100191.

Vogel JP, Gu YQ, Twigg P, Lazo GR, Laudencia-Chingcuanco D, Hayden DM, Donze TJ, Vivian LA, Stamova B, and Coleman-Derr D. 2006. EST sequencing and phylogenetic analysis of the model grass Brachypodium distachyon. *Theor Appl Genet* **113**: 186–195.

Waterhouse PM, and Helliwell CA. 2003. Exploring plant genomes by RNA-induced gene silencing. *Nat Rev Genet* **4**: 29–38.

Wesley SV, Helliwell CA, Smith NA, Wang MB, Rouse DT, Liu Q, Gooding PS, Singh SP, Abbott D, Stoutjesdijk PA, et al. 2001. Construct design for efficient, effective and high-throughput gene silencing in plants. *Plant J* **27**: 581–590.

Wisniewska J, Xu J, Seifertová D, Brewer PB, Ruzicka K, Blilou I, Rouquié D, Benková E, Scheres B, and Friml J. 2006. Polar PIN localization directs auxin flow in plants. *Science* **312**: 883.

Xu M, Zhu L, Shou H, and Wu P. 2005. A PIN1 family gene, OsPIN1, involved in auxin-dependent adventitious root emergence and tillering in rice. *Plant Cell Physiol* **46**: 1674–1681.

Zhang J, Nodzynski T, Pencík A, Rolcík J, and Friml J. 2010. PIN phosphorylation is sufficient to mediate PIN polarity and direct auxin transport. *Proc Natl Acad Sci USA* **107**: 918–922.

Zhou C, Han L, and Wang Z-Y. 2011. Potential but limited redundant roles of MtPIN4, MtPIN5 and MtPIN10/SLM1 in the development of Medicago truncatula. *Plant Signal Behav* **6**.

Zhou C, Han L, Hou C, Metelli A, Qi L, Tadege M, Mysore KS, and Wang Z-Y. 2011. Developmental analysis of a Medicago truncatula smooth leaf margin1 mutant reveals context-dependent effects on compound leaf development. *Plant Cell* **23**: 2106–2124.

Zimmermann MH, and Tomlinson PB. 1972. The Vascular System of Monocotyledonous Stems. *Botanical Gazette* **133**: 141–155.

Zimmermann W. 1952. Main results of the “thelome theory.” *Paleobotanist* **1**: 456–470.